Dynamic pair-breaking current, critical superfluid velocity, and nonlinear electromagnetic response of nonequilibrium superconductors

Ahmad Sheikhzada ●* and Alex Gurevich†

Department of Physics and Center for Accelerator Science, Old Dominion University, Norfolk, Virginia 23529, USA

We report numerical calculations of a dynamic pair-breaking current density J_d and a critical superfluid velocity v_d in a nonequilibrium superconductor carrying a uniform, large-amplitude AC current density $J(t) = J_a \sin \Omega t$ with Ω well below the gap frequency $\Omega \ll \Delta_0/\hbar$. The dependencies $J_d(\Omega, T)$ and $v_d(\Omega, T)$ near the critical temperature T_c were calculated from either the full time-dependent nonequilibrium equations for a dirty s-wave superconductor or the time-dependent Ginzburg-Landau (TDGL) equations for a gapped superconductor, taking into account the GL relaxation time of the order parameter τ_{GL} and the inelastic electron-phonon relaxation time of quasiparticles τ_E. We show that both approaches give similar frequency dependencies of $J_d(\Omega)$ and $v_d(\Omega)$ which gradually increase from their static pair-breaking GL values J_c and v_c at $\Omega\tau_E \ll 1$ to $\sqrt{2}J_c$ and $\sqrt{2}v_c$ at $\Omega\tau_E \gg 1$. Here J_d, v_d and a dynamic superheating field at which the Meissner state becomes unstable were calculated in two different regimes of a fixed AC current and a fixed AC superfluid velocity induced by the applied AC magnetic field $H = H_a \sin \Omega t$ in a thin superconducting filament or a type-II superconductor with a large GL parameter. We also calculated a nonlinear electromagnetic response of a nonequilibrium superconducting state, particularly a dynamic kinetic inductance and a dissipative quasiparticle conductivity, taking into account the oscillatory dynamics of superconducting condensate and the kinetics of quasiparticles driven by a strong AC current. It is shown that an AC current density produces multiple harmonics of the electric field, the amplitudes of the higher-order harmonics diminishing as τ_E increases.

I. INTRODUCTION

Mechanisms of the maximum superfluid velocity v_c and the DC depairing current density J_c, which a superconductor can carry in an equilibrium state, have been well established [1]. The first calculations [2] of $v_c(T)$ and $J_c(T)$ were based on the Ginzburg-Landau (GL) equations near the critical temperature $T \approx T_c$. Furthermore, $v_c(T)$ and $J_c(T)$ have been calculated in the whole temperature range $0 < T < T_c$ in the BCS model for clean [3–6] and dirty [5,6] superconductors with nonmagnetic and magnetic impurities [7] and taking into account strong electron-phonon coupling in the Eliashberg theory [8]. The DC depairing current densities have been measured for different superconducting materials [9–11]. These issues are closely related to a maximum superheating magnetic field H_s which can be sustained by a superconductor in the vortex-free Meissner state. Here $H_s(T)$ near T_c has been calculated from the GL theory [12,13] and for type-II superconductors with a large GL parameter $\kappa \gg 1$ at $T = 0$ [14] and in the entire temperature range $0 < T < T_c$ both in the clean limit [15] and for arbitrary concentrations of nonmagnetic and magnetic impurities [16]. Nonlinear screening and breakdown of superconductivity in proximity-coupled bilayers under a strong DC magnetic field have been calculated in Refs. [17–20].

Unlike the static v_c and J_c in equilibrium, the physics of the dynamic critical superfluid velocity v_d and the depairing current density J_d at which superconductivity is destroyed in a *nonequilibrium* state is not well understood. The dynamic v_d and J_d are controlled by both the nonlinear current pair-breaking effects and a complex kinetics of quasiparticles driven out of equilibrium by a time-dependent electromagnetic field [21]. For an oscillating superflow $J(t) = J_a \sin \Omega t$, the dynamic v_d and J_d depend on the frequency Ω and the relaxation time constants for the superfluid density $\tau_{\mathrm{GL}}(T)$ and quasiparticles $\tau_E(T)$. At $\Omega \ll \Delta/\hbar$ the AC field does not generate new quasiparticles which transfer the absorbed power to phonons. At $k_B T \ll \Delta$ this power transfer is mostly limited by an inelastic scattering time of quasiparticles $\tau_s(T)$ and a recombination time of Cooper pairs $\tau_r(T)$ due to electron-phonon collisions [22]:

$$\tau_r \simeq \tau_1 \left(\frac{T_c}{T}\right)^{1/2} e^{\Delta/T}, \quad \tau_s \simeq \tau_2 \left(\frac{T_c}{T}\right)^{7/2}, \quad (1)$$

where τ_1 and τ_2 are materials constants. Depending on the amplitude J_a, the distribution function of quasiparticles $f(E, t)$ can either deviate strongly from the Fermi-Dirac distribution $f_0(E)$ at $(\tau_r, \tau_s)\Omega \gg 1$ or relax to $f_0(E)$ at $(\tau_r, \tau_s)\Omega \ll 1$. Since both $\tau_r(T)$ and $\tau_s(T)$ increase as T decreases, nonequilibrium effects become more pronounced at $T \ll T_c$. By contrast, $\tau_{\mathrm{GL}}(T)$ increases as T increases and diverges at

$T = T_c$ [21],

$$\tau_{\mathrm{GL}}(T) \simeq \frac{\pi \hbar}{8 k_B (T_c - T)}, \quad T \approx T_c. \qquad (2)$$

At $T \ll T_c$ the condition $\Omega \tau_{\mathrm{GL}} \lesssim 1$ is satisfied up to 0.1–1 THz for most superconductors but breaks down at temperatures very close to T_c. For instance, at 1 GHz we have $\Omega \tau_{\mathrm{GL}}(T) \simeq 1$ at $T_c - T \simeq \pi \hbar \Omega / 8 k_B \sim 10^{-2}$ K.

The dynamics of the condensate at $\Omega \tau_{\mathrm{GL}} \ll 1$ remains nearly quasistatic if the effect of quasiparticles is weak. At $T \ll T_c$ the relaxation times $\tau_s(T)$ and $\tau_r(T)$ increase strongly as the temperature decreases so that $(\tau_r, \tau_s)\Omega \gtrsim 1$ while $\Omega \tau_{\mathrm{GL}} \ll 1$, and the AC field can produce highly nonequilibrium quasiparticles. Yet the density of quasiparticles in s-wave superconductors at $T \ll T_c$ and $\Omega \ll \Delta/\hbar$ is exponentially small as compared to the superfluid density, so the nonequilibrium quasiparticles have only a weak effect on the dynamics of the condensate which reacts almost instantaneously to $J(t)$. In this case, the dynamic v_d and J_d at $\Omega \ll \Delta/\hbar$ and $T \ll T_c$ would be close to the static v_c and J_c in thermodynamic equilibrium.

The situation changes at $T \approx T_c$ where the superfluid density becomes smaller than the density of nonequilibrium quasiparticles which significantly affect the dynamic v_d and J_d at which superconductivity breaks down. In this work we used both the time-dependent Ginzburg-Landau (TDGL) equations and a full set of nonequilibrium equations for dirty superconductors in a low-frequency ($\Omega \ll \Delta/\hbar$) field [21,23–26] to calculate the dynamic $v_d(T, \Omega)$ and $J_d(T, \Omega)$ at $T \simeq T_c$, where nonequilibrium effects are most pronounced. We consider the case of $\hbar\Omega \ll k_B T$ in which the microwave stimulation of superconductivity [27] does not happen, but the AC currents strongly affect the density of states of quasiparticles [6,28,29] and drive them out of equilibrium.

The physics of the dynamic critical velocity is relevant to many applications, for instance, microwave thin film superconducting resonators used in kinetic inductance photon detectors and astrophysical spectroscopy [30,31]. It is also essential for superconducting resonant cavities for particle accelerators, where the breakdown fields close to the thermodynamic superheating field H_s have been achieved at very high quality factors $\sim 10^{10}$ at 2 K in the Meissner state [32,33]. These cavities operate at 0.1–3 GHz much lower than the gap frequency $\Delta/h \simeq 0.8$ THz for Nb, and the dynamic superheating field H_d sets a theoretical limit of the rf breakdown. The dynamic superheating field was measured by Yogi *et al.* [34] who showed that for Sn, Pb, and In at 90–300 MHz, the breakdown field near T_c is close to $H_s(T)$. Pulse measurements [35] on Nb and Nb$_3$Sn at GHz frequencies at 2 K $< T < T_c$ have shown that the field onset of magnetic flux penetration is close to $H_s(T)$ for Nb near T_c but is smaller than $H_s(T)$ for Nb$_3$Sn at lower T.

In this work we calculate the dynamic $J_d(\Omega, T)$ and a critical phase gradient $Q_d(\Omega, T)$ of the order parameter related to v_d by $Q_d = m v_d / \hbar$, where m is the electron mass [1] for a uniform AC superflow at $T \simeq T_c$. We focus here on the maximum amplitude of the AC current density $J(t) = J_a \sin \Omega t$ which can be sustained in nonequilibrium Meissner states and do not consider nonuniform dissipative states at $J_a > J_d$ due to proliferation of phase slip centers in narrow filaments [36–38]
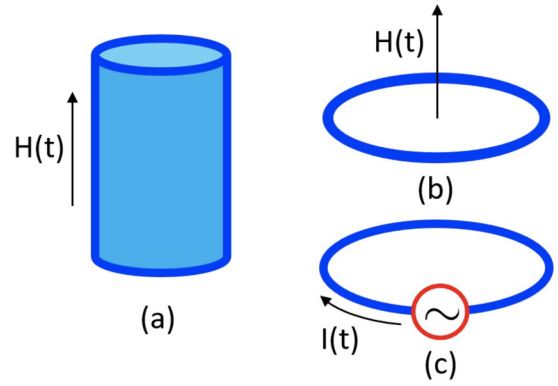

FIG. 1. Geometries for which $Q_d(\Omega, T)$ and $J_d(\Omega, T)$ are calculated: (a) A thin film cylinder in a parallel AC magnetic field, (b) a thin filament ring in a perpendicular magnetic field, and (c) a thin wire connected to an AC power supply.

or penetration of vortices in bulk superconductors above the dynamic superheating field. TDGL simulations of thin filaments have shown that J_d can approach $\sqrt{2} J_c$ at $\Omega \tau_E \gg 1$ [38], while numerical simulations of kinetic equations [25,26] have shown [39] that superconductivity can persist during short current pulses with amplitudes above the static J_c. Yet the calculations of J_d and Q_d, taking into account both the nonlinear current pair-breaking and nonequilibrium kinetics of quasiparticles, have not yet been done. We also calculate a nonlinear electromagnetic response in a nonequilibrium state at $J < J_d$ and its manifestations in the nonlinear Meissner effect, kinetic inductance and intermodulation which have been so far investigated in equilibrium superconductors [40–50].

The paper is organized as follows. In Sec. II we specify the main equations and discuss the theoretical assumptions under which the equations have been derived. These equations were solved for a uniform AC superflow in Sec. III, where the dynamic $Q_d(T, \Omega)$ and $J_d(T, \Omega)$ were calculated. In Sec. IV we address a nonlinear response and calculate the current-dependent kinetic inductance both in equilibrium and nonequilibrium states. The conclusions and broader implications of our results are presented in Sec. V.

II. MAIN EQUATIONS

We consider a dirty s-wave superconductor exposed to time-dependent electromagnetic potentials $\mathbf{A}(\mathbf{r}, t)$ and $\varphi(\mathbf{r}, t)$. The dynamic $Q_d(\Omega, T)$ and $J_d(\Omega, T)$ at $T \simeq T_c$ are calculated using the equations for the order parameter $\Psi(\mathbf{r}, t) = \Delta \exp(-i\theta)$ and the current density $\mathbf{J}(\mathbf{r}, t)$ along with a kinetic equation for the distribution function of quasiparticles [23–26]. The cases of a fixed AC superfluid velocity $v(t)$ and a fixed AC current density $J(t)$ are investigated. These cases can be realized in the geometries shown in Fig. 1, where a thin film cylinder (a) and a ring filament (b) exposed to the AC magnetic field $H(t)$ correspond to the regime of fixed $v(t)$, whereas a thin wire connected to an AC power supply shown in Fig. 1(c) or a semi-infinite superconductor with $\kappa \gg 1$ corresponds to the regime of fixed $J(t)$. It is assumed that the thickness d of films and filaments is much smaller than the magnetic penetration depth λ_L, so that the induced current

density is uniform over the cross section. We focus here on the stability of a uniform Meissner state and do not consider thermally activated or quantum proliferation of vortices or phase-slip centers [51–54] and the influence of AC current [55,56] on their dynamics at $J < J_d(\Omega, T)$, or the effects of inhomogeneities [57] and current leads on the nucleation of vortices or phase slips. The condition that vortices do not nucleate at $J \sim J_d$ requires $d \lesssim \xi(T)$, where ξ is the coherence length. It is also assumed that the magnetic flux threading the samples shown in Fig. 1(a) is much greater than the flux quantum ϕ_0 and the Little-Parks oscillations [1] are washed out. Here the self-field is smaller than the applied field by the factor $d/\lambda_L \ll 1$.

The dynamic $Q_d(\Omega, T)$ and $J_d(\Omega, T)$ for both fixed electric field and fixed current are calculated by first solving the TDGL equations. The TDGL approach is useful to address qualitative mechanisms of destruction of superconductivity by an AC current, even though the TDGL theory, strictly speaking, is not applicable for the calculations of $J_d(\Omega, T)$. We then calculate $Q_d(\Omega, T)$ and $J_d(\Omega, T)$ by solving the full set of dynamic equations of Ref. [24]. Comparing the TDGL results with a more adequate theory of Refs. [23–26] shows the effects of nonequilibrium kinetics of quasiparticles and the extent to which the TDGL approach is applicable. We then proceed with the calculations of the kinetic inductance and the nonlinear electromagnetic response in nonequilibrium states.

A. TDGL equations

Slow temporal and spatial variations of $\Psi(\mathbf{r}, t)$ and $\mathbf{J}(\mathbf{r}, t)$ in a dirty s-wave superconductor at $T \approx T_c$ can be described by the TDGL equations [25,26]:

$$\frac{\pi}{8T_c\epsilon}\left(1 + 4\tau_E^2\Delta^2\right)^{-1/2}\left(\frac{\partial}{\partial t} + 2ie\varphi + 2\tau_E^2\frac{\partial\Delta^2}{\partial t}\right)\Psi$$

$$= \left(1 - \frac{\Delta^2}{\Delta_0^2}\right)\Psi + \xi^2(\nabla - 2ie\mathbf{A})^2\Psi, \qquad (3)$$

$$\mathbf{J} = \frac{\pi\sigma_0}{4eT_c}\Delta^2\mathbf{Q} - \sigma_0\left(\nabla\varphi + \frac{\partial\mathbf{A}}{\partial t}\right). \qquad (4)$$

Here $\xi = (\pi\hbar D/8k_B T_c\epsilon)^{1/2}$ is the coherence length, $D = v_F l/3$ is diffusion constant, v_F is the Fermi velocity, l is the mean free path, $\epsilon = 1 - T/T_c$, τ_E is an energy relaxation time due to inelastic scattering of quasiparticles on phonons [21], $\Delta_0^2 = 8\pi^2 k_B^2 T_c^2\epsilon/7\zeta(3)$, $\sigma_0 = 2e^2 DN(0)$ is the normal state conductivity, $N(0)$ is the density of states on the Fermi surface, $-e$ is the electron charge, and $\mathbf{Q} = -(\nabla\theta + 2\pi\mathbf{A}/\phi_0)$ is a gauge-invariant phase gradient. Equations (3) and (4) (in which the units with $\hbar = k_B = 1$ are used) were derived from the kinetic BCS theory under the condition of local equilibrium, assuming that $\mathbf{Q}(\mathbf{r}, t)$ and $\Delta(\mathbf{r}, t)$ vary slowly over ξ_0, the diffusion length $L_E = (D\tau_E)^{1/2}$ and τ_E [21,25,26], where

$$\tau_E = \frac{8\hbar}{7\pi\zeta(3)\lambda k_B T}\left(\frac{c_s}{v_F}\right)^2\left(\frac{T_F}{T}\right)^2. \qquad (5)$$

Here c_s is the speed of longitudinal sound, λ is a dimensionless electron-phonon coupling constant, and $T_F = \epsilon_F/k_B$ is the Fermi temperature. For Pb we have [58,59] $c_s \simeq 1.32$ km/s, $v_F \simeq 1830$ km/s, $T_F = 1.1 \times 10^5$ K, $T_c = 7.3$ K, and $\lambda = 1.55$, which yields $\tau_E^{Pb}(T_c) \simeq 2.52 \times 10^{-11}$ s. For Al

with $c_s \simeq 5.1$ km/s, $v_F \simeq 2030$ km/s, $T_F = 1.36 \times 10^5$ K, $T_c = 1.2$ K, and $\lambda = 0.43$, Eq. (5) gives $\tau_E^{Al}(T_c) \simeq 3.64 \times 10^{-7}$ s.

For a uniform superflow, Eqs. (3) and (4) in the gauge $\varphi = 0$ can be written in the following dimensionless form:

$$(1 + 4\tau^2\psi^2)^{1/2}\frac{\partial\psi}{\partial t} = (1 - q^2)\psi - \psi^3, \qquad (6)$$

$$j = u\psi^2 q + \frac{\partial q}{\partial t}, \qquad (7)$$

where $\psi = \Delta/\Delta_0$, $q = Q\xi$, $\tau = \Delta_0\tau_E/\hbar$, $j = J/J_0$, t is in units of τ_{GL}, $J_0 = \sigma_0/2e\xi\tau_{GL}$, and $u = \pi^4/14\zeta(3) \approx 5.79$.

B. Nonequilibrium kinetic equations

For a uniform current flow, the full set of nonequilibrium kinetic equations [24–26] given in Appendix A can be reduced to a single kinetic equation for the odd in energy E part of the quasiparticle distribution function $f(E, t)$, and dynamic equations for $\psi(t)$ and $j(t)$:

$$R_2\frac{\partial f}{\partial E}\frac{\partial\psi}{\partial t} + N_1\left(\frac{\partial}{\partial t} + \frac{s}{2\tau}\right)\delta f = \frac{N_2 R_2}{s}\frac{\partial f}{\partial E}\frac{\partial q^2}{\partial t}, \qquad (8)$$

$$\frac{\partial\psi}{\partial t} - \frac{1}{\epsilon}\int_0^\infty R_2\delta f\, dE = (1 - q^2)\psi - \psi^3, \qquad (9)$$

$$j = u\psi^2 q + \frac{\partial q}{\partial t}\int_0^\infty \left(N_1^2 + N_2^2\right)\frac{\partial f}{\partial E}dE$$

$$+ 2qs\int_0^\infty N_2 R_2\delta f\, dE, \quad s = (u/\epsilon)^{1/2}. \qquad (10)$$

Here $\delta f(E, t) = f(E, t) - f_0(E)$, $f_0 = \tanh(E/2T)$, the quasiparticle energy E and temperature T are in units of Δ_0, and the scaling factor $(u/\epsilon)^{1/2} = 2\tau_{GL}\Delta_0/\hbar$ results from the same normalization of the parameters as in Eqs. (6) and (7). If $\Omega\tau_{GL} \ll 1$ the spectral functions N_1, N_2, R_1, and R_2 are defined by the normal $\alpha(E) = N_1(E) + iR_1(E)$ and anomalous $\beta(E) = N_2(E) + iR_2(E)$ Green's functions which satisfy the quasistatic Usadel equation for 1D current flow [25,26]:

$$\left(\frac{1}{2\tau} - iE\right)\beta + \frac{q^2}{2}\alpha\beta = \psi\alpha, \qquad (11)$$

where $\alpha^2 + \beta^2 = 1$. Equation (11) reduces to a quartic equation for α, the solutions of which are given in Appendix A. The term $1/2\tau$ in Eq. (11) defines a finite quasiparticle lifetime due to scattering on phonons, resulting in subgap states at $|E| < \psi$. We do not consider here other contributions to the subgap states [60–62].

We solved the integro-differential Eqs. (8)–(10) numerically using the method of lines [63]. By discretizing the energy, Eqs. (8)–(10) were reduced to coupled ordinary differential equations in time which were solved by the Adams-Bashforth-Moulton method [64] with the error tolerances below 10^{-6}. Results of the calculations of the dimensionless $j_d = J_d/J_0$ and $q_d = Q_d\xi$ as functions of the dimensionless frequency $\omega = \Omega\tau_{GL}$ and the quasiparticle relaxation time $\tau = \tau_E\Delta_0/\hbar$ are given below.
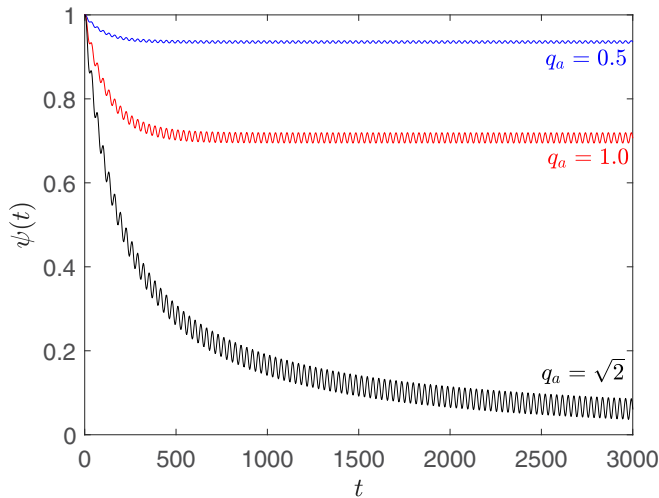
FIG. 2. Dynamics of $\psi(t)$ calculated at $q = q_a \sin \omega t$, $\tau = 100$, and $\omega = 0.1$. Here $\psi(t)$ eventually vanishes at $q_a = \sqrt{2}$.

III. DYNAMIC PAIR-BREAKING CURRENT

A. TDGL results

The stationary Eqs. (6) and (7) have the solution $\psi = 0$ at $q > 1$ and $\psi = \sqrt{1 - q^2}$ at $q < 1$. Stability of this solution with respect to small perturbations $\delta\psi(t)$ and $\delta q(t)$ depends on the way by which the superflow is generated. In the regime of fixed q the stationary solution $\psi(q)$ is stable in the whole region of $q < q_c = 1$, but in the regime of fixed j the solution $\psi(q)$ is stable if q is smaller than $q_c = 1/\sqrt{3}$ at which $j = uq(1 - q^2)$ reaches maximum [1,2]. This gives the GL depairing current density $j_c = 2u/3\sqrt{3}$ above which $\psi(j)$ drops from $\psi(j_c) = \sqrt{2/3}$ to zero.

1. Fixed Q(t)

Figure 2 shows $\psi(t)$ calculated from Eq. (6) with $q(t) = q_a \sin \omega t$ at $\omega = \Omega \tau_{GL} = 0.1$, $\tau = 100$, and the initial condition $\psi(0) = 1$. Here $\psi(t)$ relaxes after a transient period $t \gtrsim \sqrt{1 + 4\tau^2}$ to an oscillating steady state with a nonzero mean $\langle\psi\rangle$ if $q_a < q_d(\omega, T)$ or to the normal state with $\psi(t) = 0$ at $t \gg 1$ if $q_a > q_d(\omega, T)$. The mean $\langle\psi(q_a)\rangle$ decreases with q_a and vanishes at $q_a = q_d$.

The calculated dependencies of q_d on ω and τ are shown in Fig. 3. Here $q_d(\tau)$ at $\omega = 0.01$ increases from $q_d(0) \approx 1.097$ at $\tau = 0$ to $q_d(\tau) \to \sqrt{2}$ at $\tau \gg 1$. At higher frequency $\omega = 0.1$, the dynamic $q_d(\tau)$ is nearly equal to $\sqrt{2}$ at all τ. However, if τ is fixed but the frequency changes, $q_d(\omega)$ varies from $q_c = 1$ at $\omega = 0$ to $q_d(\omega) \to \sqrt{2}$ at $\omega\sqrt{1 + 4\tau^2} \gg 1$. The universal value of $q_d = \sqrt{2}$ is achieved at $\omega\tau \gtrsim 1$, that is, for Ω exceeding a crossover frequency $\Omega_c \simeq \hbar/\tau_{GL}\Delta_0\tau_E$ given by

$$\Omega_c \simeq \frac{k_B}{\Delta_0\tau_E}(T_c - T) \sim \frac{k_B T^3}{\hbar T_D^2}\sqrt{1 - \frac{T}{T_c}}, \qquad (12)$$

where T_D is the Debye temperature. Here $\Omega_c(T)$ vanishes at T_c, reaches maximum $\Omega_m = \Omega_c(6T_c/7)$ at $T/T_c \approx 0.86$ and decreases with T at $T < 0.8T_c$, as shown in Fig. 4.
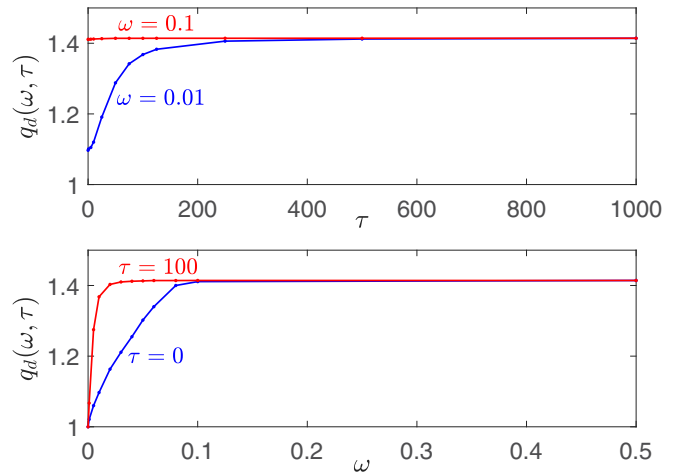

FIG. 3. The calculated dependencies of q_d on τ (top) and ω (bottom). Here $q_d \to \sqrt{2}$ at $\omega\tau \gtrsim 1$.

The increase of $Q_d(\Omega, T)$ at $\Omega \gtrsim \Omega_c(T)$ by the factor $\sqrt{2}$ can be understood as follows. As follows from Fig. 2, $\psi(t)$ oscillates rapidly around a mean $\langle\psi\rangle$. Here $\langle\psi\rangle \simeq \sqrt{1 - \langle q^2\rangle}$ is determined by Eq. (6) with the time-averaged $\langle q^2(t)\rangle = q_a^2/2$ so $\langle\psi\rangle$ vanishes at $q_a = \sqrt{2}$. A small-amplitude AC correction $\delta\psi(t)$ was calculated in Appendix B. The superconducting state remains stable in the whole region $0 < q_a < q_d$.

The temperature dependence of $Q_d(\Omega, T)$ shown in Fig. 5 is affected by the ratio $\Omega/\Omega_c(T)$. If $\Omega > \Omega_m = \Omega_c(6T_c/7)$ (see Fig. 4), the dynamic $Q_d(T) \to \sqrt{2}/\xi(T)$ has the same temperature dependence as the static $Q_c = 1/\xi(T)$. However, if $\Omega \ll \Omega_m$, we obtain that $Q_d(T) \to \xi_0^{-1}\sqrt{2(1 - T/T_c)}$ at T close to T_c and crosses over to the static $Q_c(T)$ at lower T. There is also a range of frequencies $\Omega < \Omega_m$ but $\Omega \gtrsim \Omega_c(T_c/2)$ (see Fig. 4) in which $Q_d(T)$ evolves from $\sqrt{2}Q_c(T)$ at $T \to T_c$ to $Q_d \simeq Q_c(T)$ at $T \lesssim 0.8T_c$ and back to $\simeq \sqrt{2}Q_c(T)$.
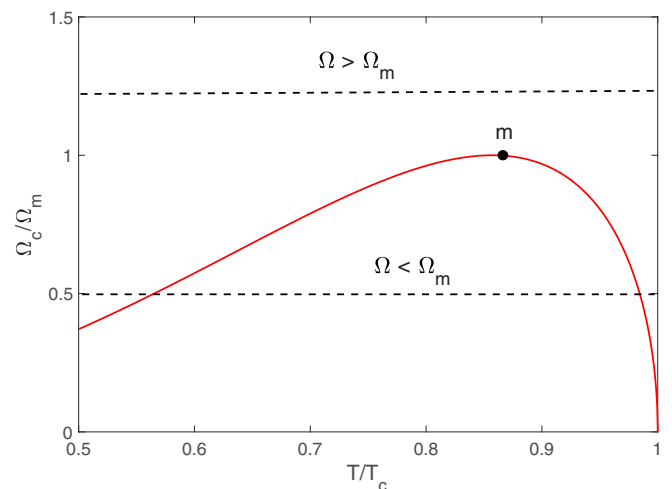

FIG. 4. Temperature dependence of $\Omega_c(T)$. The dashed lines show the levels of fixed Ω at $\Omega > \Omega_m$ and $\Omega < \Omega_m$, where Ω_m is the maximum value of $\Omega_c(T)$ corresponding to the point m.
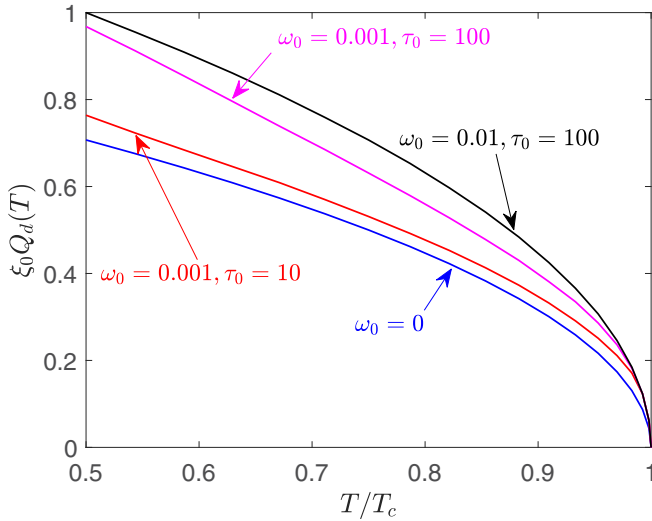
FIG. 5. $Q_d(T)$ calculated for different values of $\omega_0 = \pi\hbar\Omega/8k_BT_c$ and $\tau_0 = \tau_E(T_c)\Delta_0(0)$, where $\Delta_0^2(0) = 8\pi^2T_c^2/7\zeta(3)$. Here the dynamic $Q_d = \sqrt{2(1 - T/T_c)}/\xi_0$ at $\Omega \gg \Omega_c(T)$ has the same temperature dependence as the static $Q_c = \sqrt{1 - T/T_c}/\xi_0$. If $\Omega \sim \Omega_c(T)$ the behavior of $Q_d(T)$ is affected by the temperature dependence of $\tau_E(T)$, as shown for the case of $\omega_0 = 0.001$ and $\tau_0 = 100$.

2. Fixed J(t)

We calculated $\psi(t)$ at a fixed $j(t) = j_a \sin\omega t$ by solving the coupled Eqs. (6) and (7). The GL DC depairing current density $j_c = 2u/3\sqrt{3} \approx 2.228$ is reached at $q = 1/\sqrt{3}$ and $\psi^2 = 2/3$, while at $q > 1/\sqrt{3}$ the superconducting state becomes unstable and $\psi(q)$ vanishes abruptly [1]. This feature is characteristic of the AC current as well, which makes it different from the regime of fixed $q(t)$. For instance, Fig. 6 shows $\psi(t)$ calculated at $\tau = 10$ and $\omega = 0.1$. At $j_a = 1.38j_c$
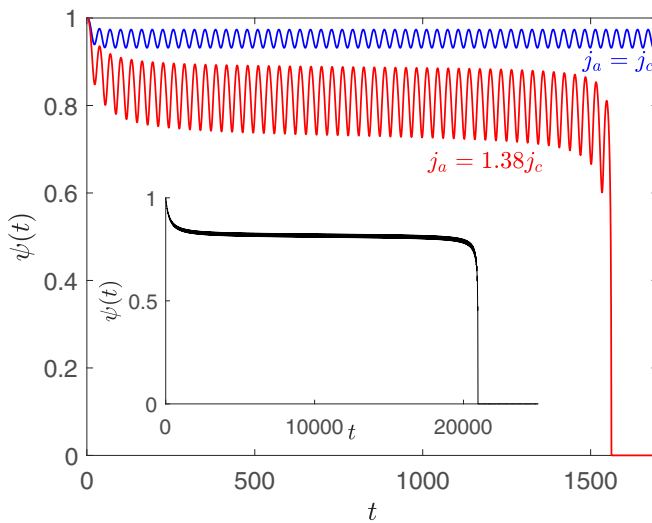

FIG. 6. Dynamics of $\psi(t)$ calculated at $j = j_a \sin\omega t$, $\omega = 0.1$, $\tau = 10$, and different amplitudes j_a. At $j_a = j_c$, the superconducting state still exists, but once j_a reaches the dynamic pair-breaking current $j_d = 1.38j_c$, $\psi(t)$ vanishes. The inset shows $\psi(t)$ calculated at $\tau = 100$ at $j_a = \sqrt{2}j_c$ and $\omega = 0.1$.
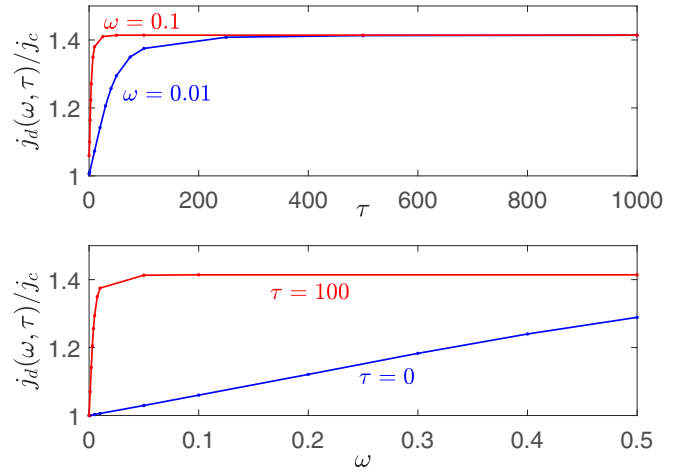

FIG. 7. Dynamic pair-breaking current j_d as a function of τ (top) and ω (bottom). Here $j_d(\omega, \tau) \to \sqrt{2}j_c$ at $\omega\tau \gg 1$.

the order parameter abruptly vanishes after a transient period. For large τ, this transition to the normal state occurs at $j_a = \sqrt{2}j_c$, as shown in the inset for $\tau = 100$ and $\omega = 0.1$. Here the dynamic pair-breaking current $j_d(\omega, \tau)$ shown in Fig. 7 exhibits similar dependencies on ω and τ as $q_d(\omega, \tau)$ at a fixed $q(t)$. If $\omega\tau \gtrsim 1$ both the dynamic $j_d(\omega, \tau)$ and $q_d(\omega, \tau)$ are larger by the factor $\sqrt{2}$ than their respective GL values.

The temperature dependence of $J_d(\Omega, T)$ is affected by the temperature dependencies of $\tau(T)$ and $\Omega_c(T)$. At $T \to T_c$ and $\Omega \gtrsim \Omega_c(T)$ the dynamic pair-breaking current J_d is $\sqrt{2}$ times larger than the static $J_c(T)$ and is independent of τ. As T decreases $J_d(\Omega, T)$ can evolve to $J_c(T)$ at temperatures for which $\Omega \lesssim \Omega_c(T)$. This behavior of $J_d(\Omega, T)$ is illustrated in Fig. 8.
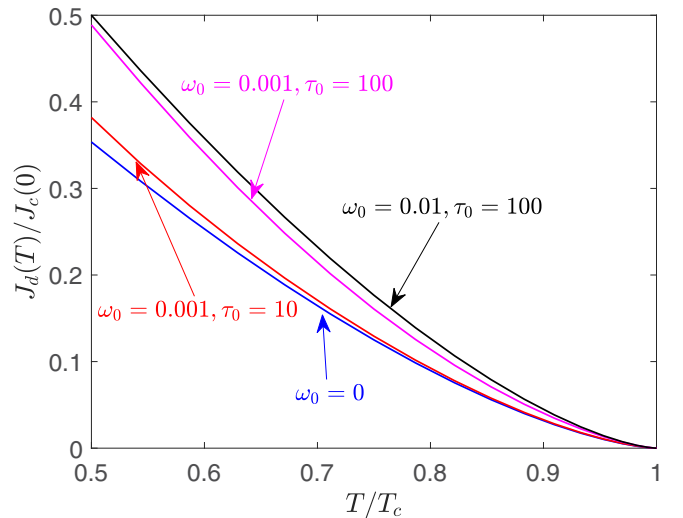

FIG. 8. $J_d(T)$ calculated for different values of $\omega_0 = \pi\hbar\Omega/8k_BT_c$ and $\tau_0 = \tau_E(T_c)\Delta_0(0)$, where $\Delta_0^2(0) = 8\pi^2T_c^2/7\zeta(3)$. Here the dynamic $J_d = \sqrt{2}J_c(0)(1 - T/T_c)^{3/2}$ at $\Omega \gg \Omega_c(T)$ has the same temperature dependence as the static $J_c = J_c(0)(1 - T/T_c)^{3/2}$. At $\Omega \sim \Omega_c(T)$ the behavior of $J_d(T)$ is affected by the temperature dependence of $\tau_E(T)$, as shown for the case of $\omega_0 = 0.001$ and $\tau_0 = 100$.
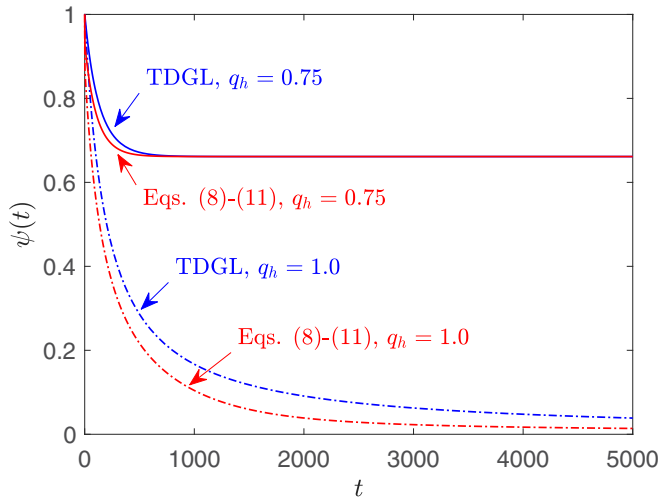
FIG. 9. Comparison of $\psi(t)$ calculated from the TDGL equation (6) and the full nonequilibrium equations (8)–(11) for $q(t) = q_h \tanh t$ at $q_h = 0.75$ and $q_h = 1$. Here we took $\tau(T) = 100$ and $T = 0.9T_c$.

B. $Q_d(T, \Omega)$ and $J_d(T, \Omega)$ calculated from the full set of nonequilibrium equations

The TDGL calculations of $q_d(T, \omega)$ and $j_d(T, \omega)$ give a qualitative picture of dynamic pair breaking, although Eqs. (6) and (7) are not really applicable at $J \simeq J_d$. Indeed, the dynamic terms in Eqs. (6) and (7) were derived from the BCS kinetic theory, assuming weak pair breaking and local equilibrium in which $Q\xi \ll 1$ and $\Delta(\mathbf{r}, t)$ varies slowly over the diffusion length $L_E = (D\tau_E)^{1/2}$ and the energy relaxation time τ_E [25,26]. Those conditions break down at $Q \simeq Q_c \sim \xi^{-1}$ and $\Omega \gtrsim \tau_{GL}^{-1}$, so in this section we calculate $\psi(t)$, $q_d(T, \omega)$, and $j_d(T, \omega)$ from Eqs. (8)–(10) which take into account both the dynamic current pair breaking and nonequilibrium kinetics of quasiparticles.

Consider first solutions of Eqs. (8)–(11) at $\tau(T) = 100$ and $T = 0.9T_c$ for a superflow $q(t) = q_h \tanh t$ which was gradually turned on at $t = 0$. As shown in Fig. 9, the qualitative behavior of $\psi(t)$ calculated from Eqs. (8) and (9) turns out to be similar to that of TDGL, except that the nonequilibrium integral term in Eq. (9) accelerates relaxation of $\psi(t)$ at $q_h \simeq 1$. In both cases superconductivity is destroyed at $q_h = 1$.

Shown in Fig. 10 are snapshots of a nonequilibrium part of the distribution function $\delta f(E, t)$ induced by the stepwise $q(t)$. Here the magnitude of $\delta f(E, t)$ calculated at $\tau = 100$ increases as q_h increases but remains relatively small up to $q_h = 1$. As the quasiparticle relaxation time τ increases, the magnitude of $\delta f(E, t)$ also increases. The peak in $\delta f(E, t)$ shifts to lower energies as q_h increases, consistent with the decrease of the quasiparticle gap due to the DC current pair breaking.

C. Fixed $Q(t)$

Solutions of Eqs. (8) and (9) with $q(t) = q_a \sin \omega t$ are shown in Fig. 11 along with the TDGL results obtained for the same input parameters. At $q_a = 1$ the order parameters $\psi(t)$ oscillate around nearly the same mean values $\langle \psi \rangle$ but
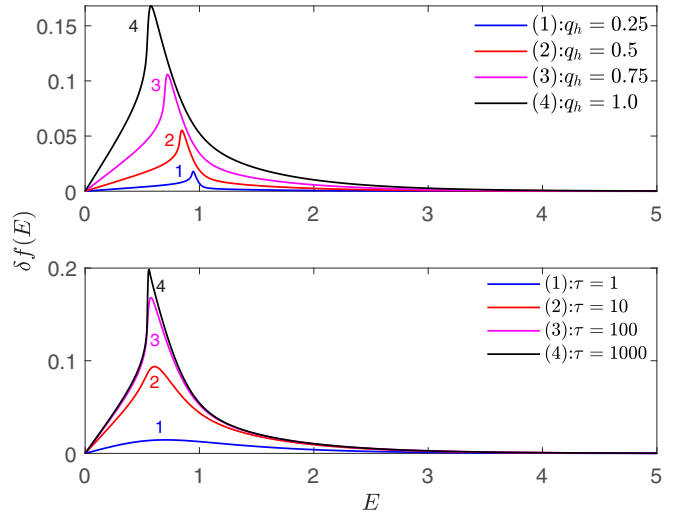

FIG. 10. The nonequilibrium correction $\delta f(E)$ at the times when the magnitude $\delta f(E, t)$ reaches maximum after the stepwise increase of $q(t)$. Taking $T = 0.9T_c$, here the top panel shows $\delta f(E, t)$ calculated for different q_h at $\tau = 100$ and the bottom panel shows $\delta f(E, t)$ calculated for different values of τ at $q_h = 1$.

the amplitude of oscillations $\delta\psi(t)$ calculated from Eqs. (8) and (9) is noticeably larger than the TDGL $\delta\psi(t)$. Relaxation of $\psi(t)$ from the initial value $\psi(0) = 1$ to the steady-state oscillations described by Eqs. (8) and (9) is also faster than the TDGL transient time, consistent with the above results for $q(t) = q_h \tanh t$ shown in Fig. 9. These features become more pronounced at the dynamic critical momentum $q_d \simeq \sqrt{2}$ at $\omega\tau \gg 1$, where the amplitudes of oscillations $\delta\psi(t)$ grow significantly larger so that $\psi(t)$ touches zero but then recovers. Yet, despite a rather different dynamics of $\psi(t)$ described by Eqs. (8) and (9) and the TDGL equations, superconductivity gets destroyed at the same critical value $q_d \to \sqrt{2}$ at $\tau = 100$ and $\omega = 0.1$ in both cases. The calculated dependencies of
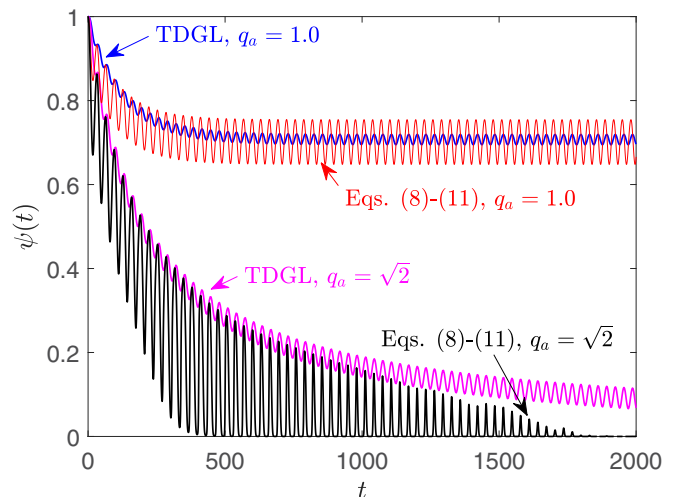

FIG. 11. Comparison of $\psi(t)$ calculated from the TDGL equations and Eqs. (8) and (9) for $q(t) = q_a \sin \omega t$, $\tau = 100$, $\omega = 0.1$, and $T = 0.9T_c$.
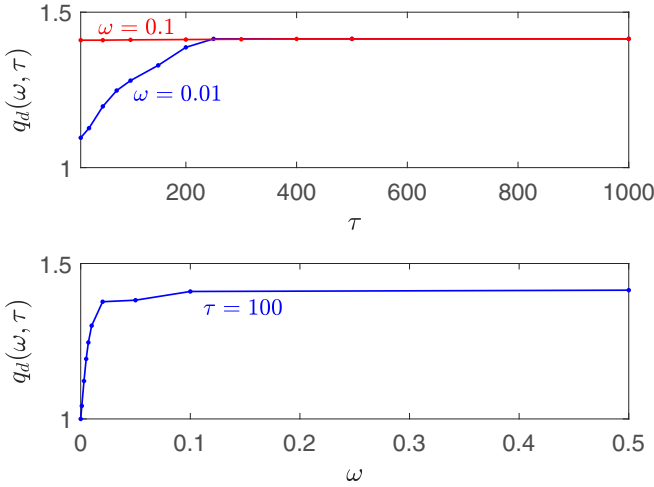
FIG. 12. Dynamic $q_d(\omega, \tau)$ as functions of τ (top) and ω (bottom) calculated from Eqs. (8) and (9) at $T = 0.9T_c$.

q_d on τ and ω shown in Fig. 12 appear similar to the TDGL results shown by Fig. 3.

Our solutions of Eqs. (8) and (9) have revealed a dynamic state in which $\psi(t)$ periodically vanishes but then recovers to $\psi(t) \sim 1$. This state appears as the frequency decreases, as shown in Fig. 13. For instance, in the case of $\omega = 0.1$ and $\tau = 10$ shown in the top panel Fig. 13, $\psi(t)$ drops down to $\sim 2 \times 10^{-3}$ at the minimum but remains finite. As $\psi(t)$ goes through the minimum the amplitude of $\delta f(E, t)$ decreases and changes sign. However, at $\omega = 0.01$ in the bottom panel, $\psi(t)$ at the minimum drops below the numerical tolerance level of $\sim 10^{-7}$ during a significant portion of the AC period. This case corresponds to a true transition to the normal state with $\psi = 0$ in which all terms in Eq. (9) vanish and Eq. (8) describes an exponential relaxation of $\delta f(E, t) \propto \exp(-ts/2\tau)$ until the superconductivity recovers as $q(t)$ decreases. This behavior is physically transparent: at very low frequencies the quasistatic
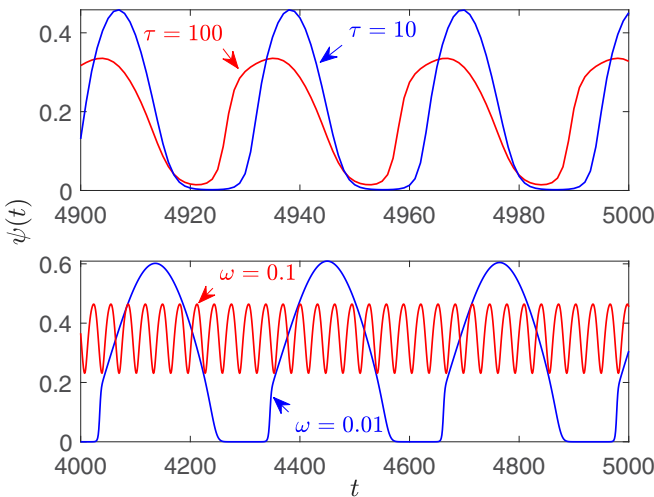

FIG. 13. Steady state oscillations of $\psi(t)$ calculated from Eqs. (8) and (9) at $T = 0.9T_c$ with $q = q_a \sin \omega t$ for different τ at $\omega = 0.1$ and $q_a = 1.35$ (top) and different ω at $\tau = 100$ and $q_a = 1.30$ (bottom).
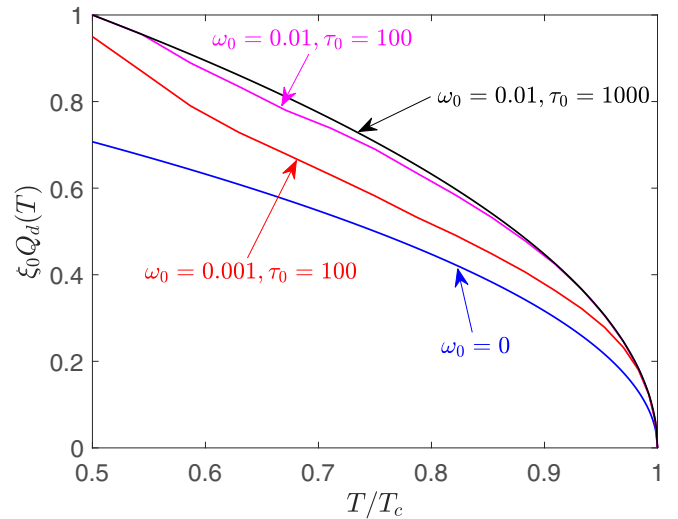

FIG. 14. $Q_d(T)$ calculated from Eqs. (8) and (9) for different values of $\omega_0 = \pi \hbar \Omega / 8 k_B T_c$ and $\tau_0 = \tau_E(T_c) \Delta_0(0)$, where $\Delta_0^2(0) = 8\pi^2 T_c^2 / 7\zeta(3)$. The dynamic $Q_d = \sqrt{2(1 - T/T_c)}/\xi_0$ at $\Omega \gg \Omega_c(T)$ has the same temperature dependence as the static $Q_c = \sqrt{1 - T/T_c}/\xi_0$. If $\Omega \sim \Omega_c(T)$ the behavior of $Q_d(T)$ is affected by the temperature dependence of $\tau_E(T)$, as shown for the case of $\omega_0 = 0.001$ and $\tau_0 = 100$.

$\psi(t)$ is determined by the instantaneous $q(t) = q_a \sin \omega t$, resulting in periodic transitions to the normal state and the subsequent recovery of superconductivity once $|q(t)|$ exceeds 1. At higher frequencies $\omega \gtrsim 0.1$, the superconducting state does not have enough time to disappear during the parts of the AC period in which $|q(t)| > 1$, so that $\psi(t)$ at the minimum remains finite all the way to $q \to q_d$.

The calculated $Q_d(T)$ curves shown in Fig. 14 are similar to the TDGL results but generally fall below them: $Q_d(\Omega, T) \to \sqrt{2}Q_c = \sqrt{2(1 - T/T_c)}$ at $\Omega \gtrsim \Omega_c(T)$ but $Q_d(\Omega, T) \to Q_c(T)$ at $\Omega \ll \Omega_c(T/2)$. The temperature dependence of $\tau(T) \propto T^{-3}$ results in a crossover of $Q_d(T, \Omega)$ from $Q_c(T)$ to $\sqrt{2}Q_c(T)$ as T decreases.

D. Fixed $J(t)$

Solutions of Eqs. (8)–(10) for $j = j_a \sin \omega t$, $\omega = 0.1$, at $\tau = 10$ and $\tau = 100$ shown in Fig. 15 are qualitatively similar to that of $\psi(t)$ for a fixed $q(t)$. Here $\psi(t)$ vanishes abruptly at $j_a = j_d(\omega, T)$, the amplitude of oscillations of $\psi(t)$ essentially depends on ω and τ, as shown in Fig. 16. The calculated $j_d = 1.35 j_c$ at $\tau(T) = 10$ turned out to be slightly smaller than the TDGL value, but at $\tau(T) = 100$ both TDGL theory and Eqs. (8)–(10) give the same $j_d = \sqrt{2} j_c$. The dependencies of $j_d(\omega, \tau)$ on τ and ω shown in Fig. 17 appear similar to those for $q_d(\omega, \tau)$ in Fig. 12 and clearly demonstrate that $j_d \to \sqrt{2} j_c$ at $\omega \tau \gg 1$. The temperature dependence of $J_d(\Omega, T)$ shown in Fig. 18 is similar to the TDGL results only at $T \to T_c$: $J_d(\Omega, T) \to \sqrt{2} J_c(0)(1 - T/T_c)^{3/2}$ at $\Omega \gtrsim \Omega_c(T)$ and $J_d(\Omega, T) \to J_c(T)$ at $\Omega < \Omega_c(T)$. As T decreases, the $J_d(\Omega, T)$ curves tend toward $J_c(T)$ even at $\Omega > \Omega_c(T)$.
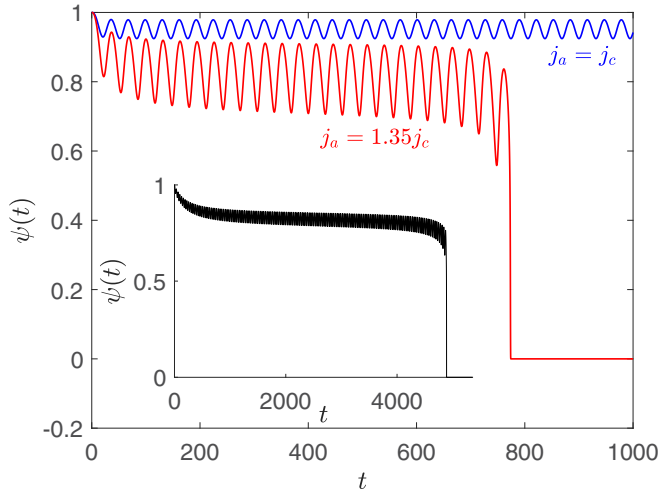
FIG. 15. Dynamics of $\psi(t)$ calculated at $j = j_a \sin \omega t$, $\omega = 0.1$, $\tau = 10$, $j_a = j_c$ and the critical current $j_a = 1.35 j_c$ at which $\psi(t)$ vanishes abruptly. The inset shows $\psi(t)$ calculated at $\tau = 100$, $\omega = 0.1$ and $j_a = \sqrt{2} j_c$. All calculations were performed at $T = 0.9 T_c$.

IV. NONLINEAR ELECTROMAGNETIC RESPONSE

In this section we address an electromagnetic response of a nonequilibrium superconductor. For a nearly uniform current considered here, the linear response is quantified by a frequency-dependent complex conductivity,

$$\mathbf{J} = (\sigma_1 - i\sigma_2)\mathbf{E}, \qquad (13)$$

where $\sigma_1(\Omega)$ describes a dissipative quasiparticle response, $\sigma_2(\Omega) = 1/\mu_0 \Omega \lambda_L^2$ accounts for the Meissner effect, and λ_L is the London penetration depth. Here σ_2 also determines the kinetic inductance $\mathcal{L}_k = (d\Omega\sigma_2)^{-1} = \mu_0 \lambda_L^2/d$ per unit length of a film of thickness d [46–50]. Using $\lambda_L^2(T) = 2\hbar k_B T_c/\pi \mu_0 \sigma_0 \Delta_0^2$ near T_c [21] yields

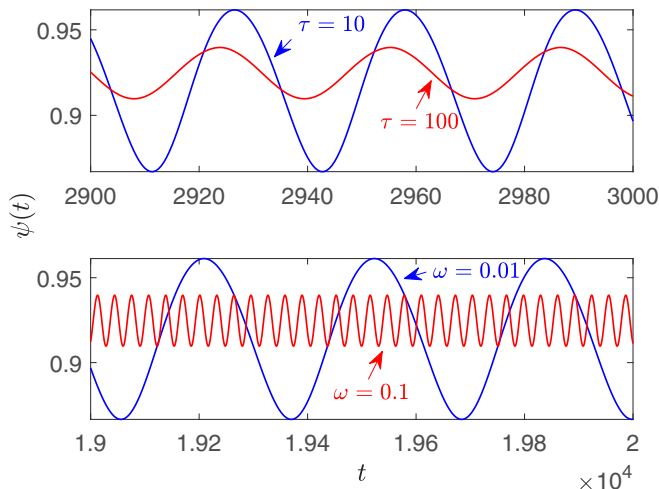$$\mathcal{L}_k = \frac{2\hbar k_B T_c}{\pi \sigma_0 d \Delta^2}. \qquad (14)$$

FIG. 16. Steady state oscillations of $\psi(t)$ calculated at $T = 0.9 T_c$, $j = j_a \sin \omega t$, $j_a = 1.20 j_c$, and different τ at $\omega = 0.1$ (top) and different ω at $\tau = 100$ (bottom).
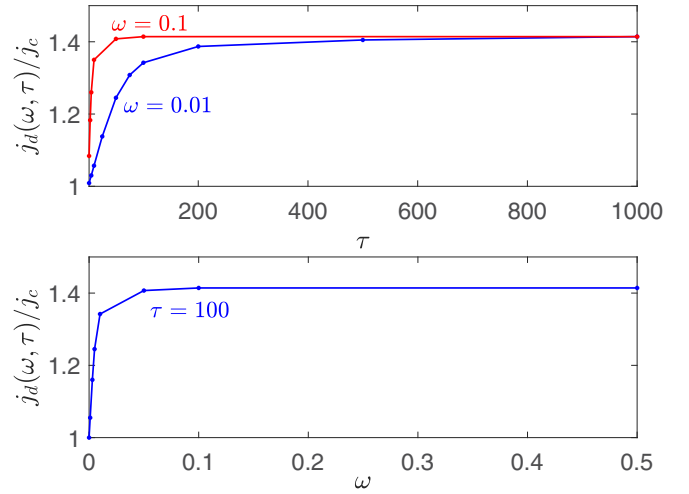

FIG. 17. Calculated dependencies of $j_d(\omega, \tau)$ on τ (top) and ω (bottom) at $T = 0.9 T_c$. Here j_d levels off at $\sqrt{2} j_c$ at $\omega\tau \gtrsim 1$.

At high current densities the conductivity $\sigma = \sigma_1 - i\sigma_2$ depends on $Q(t)$, causing the nonlinear Meissner effect, intermodulation and generation of higher order harmonics of the electric field $E(t)$ in response to the AC current $J(t) = J_a \sin \Omega t$ [40–45]. Defining the kinetic inductance by Eq. (14), where $\Delta(t)$ is given by the solutions of Eqs. (6) or Eqs. (8) and (9), we can expect strong oscillations of $\mathcal{L}_k(t)$ at large J_a due to the nonequilibrium current pair breaking. Shown in Fig. 19 is the dynamics of $\mathcal{L}_k(t)$ calculated at a fixed $q(t) = q_a \sin \omega t$ with $q_a = 0.9\sqrt{2}$, $\omega = 0.01$, and $\tau = 100$. Here the amplitudes of $\mathcal{L}_k(t)$ increase with q_a and diverge at $q_a \to q_d$, the peaks in $\mathcal{L}_k(t)$ getting higher as $\omega\tau$ decreases. Figure 19 also shows that the amplitudes of $\mathcal{L}_k(t)$ calculated from the full Eqs. (8)–(11) can be orders of magnitude higher as compared
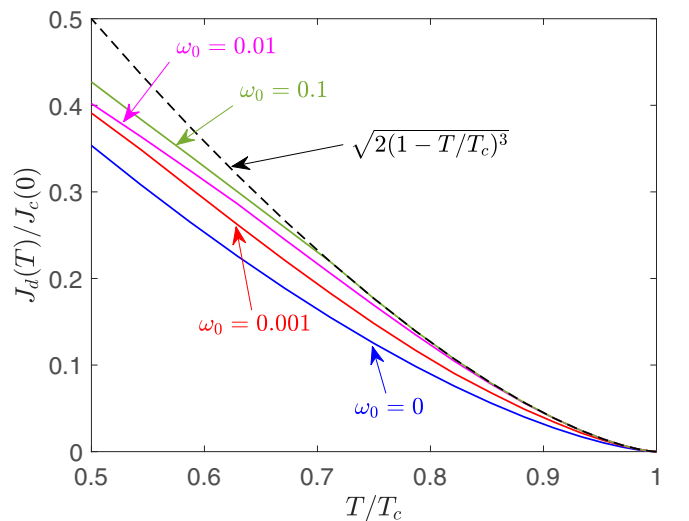

FIG. 18. $J_d(T)$ calculated from Eqs. (8)–(11) for $\tau_0 = 100$ at different $\omega_0 = \pi\hbar\Omega/8k_B T_c$ where $\tau_0 = \tau_E(T_c)\Delta_0(0)$, and $\Delta_0^2(0) = 8\pi^2 T_c^2/7\zeta(3)$. As $\Omega \gg \Omega_c(T)$, we have $J_d(T) = J_c(0)\sqrt{2}(1 - T/T_c)^{3/2}$ at $T \to T_c$, however as T decreases a crossover to $J_c(T)$ occurs even at $\Omega \geqslant \Omega_c(T)$.
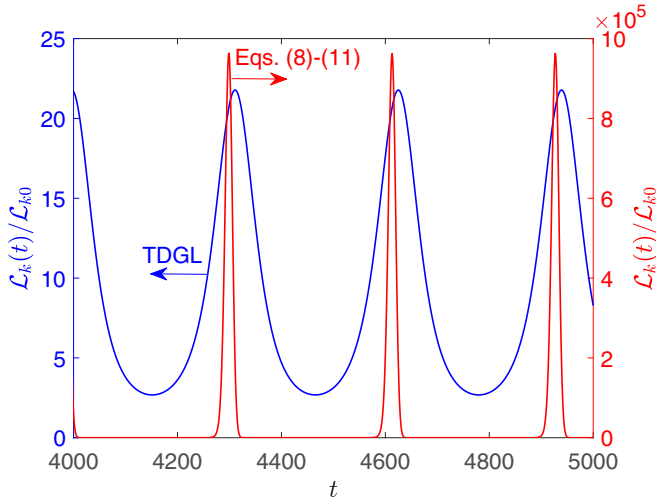
FIG. 19. Dynamics of $\mathcal{L}_k(t)$ in units of $\mathcal{L}_{k0} = \pi\sigma_0 d\Delta_0^2/2\hbar k_B T_c$ calculated from: (a) Eq. (6) and (b) Eqs. (8)–(11) at $T = 0.9T_c$ and $q(t) = q_a \sin\omega t$ with $q_a = 0.9\sqrt{2}$, $\omega = 0.01$, and $\tau = 100$. Notice large-amplitude oscillations of $\mathcal{L}_k(t)$ at small $\omega\tau$ and large q_a, the peaks in $\mathcal{L}_k(t)$ calculated from Eqs. (8)–(11) can be orders of magnitude larger than those obtained from Eq. (6).

to the TDGL results. This reflects larger amplitudes of oscillations of $\psi(t)$ calculated from Eqs. (8)–(11) and discussed above (see Fig. 11).

Shown in Fig. 20 is $\mathcal{L}_k(t)$ calculated from Eqs. (6) and (7) and Eqs. (8)–(11) at a fixed AC current $j = j_a \sin\omega t$ and $\tau = 100$. Here $\mathcal{L}_k(t)$ can exhibit large-amplitude oscillations at small $\omega\tau$. The amplitudes of $\mathcal{L}_k(t)$ calculated from Eqs. (8)–(11) are larger than the TDGL results, although not by orders of magnitude.

The above calculations of $\mathcal{L}_k(t)$ pertain to low frequencies $\omega\tau \ll 1$ at which $\mathcal{L}_k(t)$ follows instantaneously to the time-varying order parameter $\Psi(t)$. Generally, the nonlinear electromagnetic response at a fixed $q(t) = q_a \sin\omega t$ causes

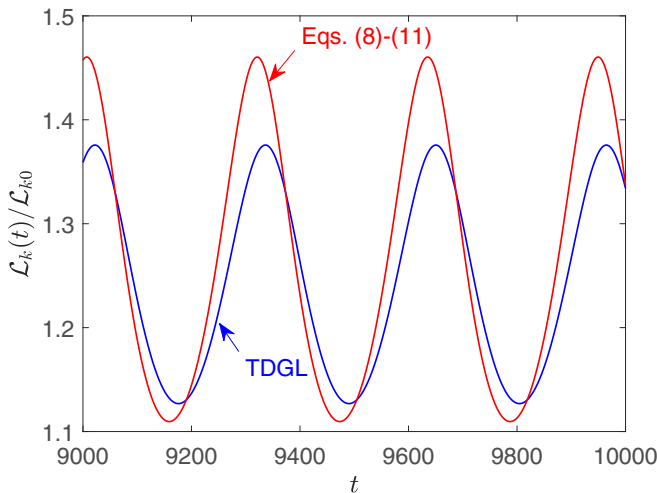

FIG. 20. Dynamics of $\mathcal{L}_k(t)$ calculated for a fixed current $j(t) = j_a \sin\omega t$ with $j_a = 0.9\sqrt{2}j_c$, $\omega = 0.01$, and $\tau = 100$ using: (a) Eqs. (6) and (7) and (b) Eqs. (8)–(11) at $T = 0.9T_c$.
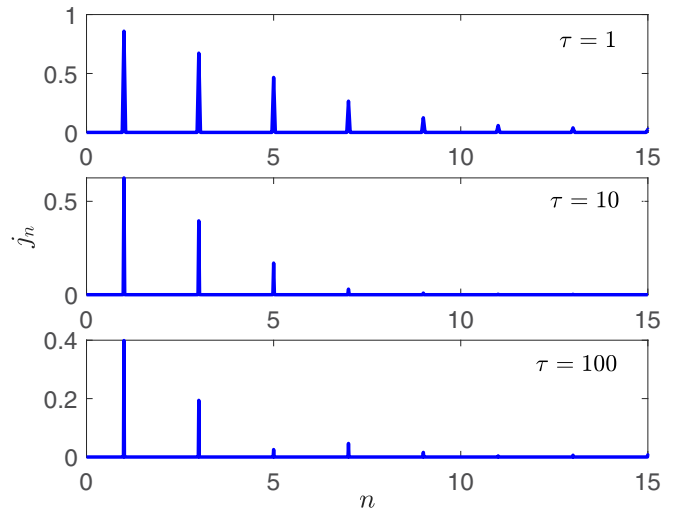

FIG. 21. Fourier spectra of the current amplitudes $j_n = \sqrt{j_{1n}^2 + j_{2n}^2}$ caused by $q(t) = q_a \sin\omega t$ calculated from Eqs. (8)–(10) for different τ at $T = 0.9T_c$, $q_a = 0.95\sqrt{2}$, and $\omega = 0.1$. The Fourier amplitudes are peaked at $\omega_n = n\omega$ with $n = 1, 3, 5, \ldots$.

generation of multiple current harmonics:

$$j(t) = \sum_n [j_{1n} \sin\omega_n t + j_{2n} \cos\omega_n t]. \tag{15}$$

Likewise, the AC current $j = j_a \sin\omega t$ produces multiple harmonics of the electric field $\varepsilon = \dot{q}$:

$$\varepsilon(t) = \sum_n [\varepsilon_{1n} \sin\omega_n t + \varepsilon_{2n} \cos\omega_n t]. \tag{16}$$

Here the frequencies ω_n and the Fourier amplitudes $j_{1n}(q_a)$, $j_{2n}(q_a)$, $\varepsilon_{1n}(j_a)$, and $\varepsilon_{2n}(j_a)$ are to be calculated self-consistently from Eqs. (8)–(10), as shown below.

A. Fixed $q(t)$

Shown in Fig. 21 are the current Fourier spectra calculated at different τ at $q_a = 0.95\sqrt{2}$ and $\omega = 0.1$. Here the multimode spectrum of $j(\omega)$ consisting of equidistant peaks at $\omega_n = n\omega$, $n = 1, 3, 5, \ldots$ changes markedly as τ increases and the amplitudes of high-frequency harmonics diminish. The latter is consistent with the results of the previous sections which showed that at $\omega\tau \gg 1$ the amplitude of oscillations of superfluid density responsible for the generation of higher harmonics diminishes and the fundamental harmonic in $j(t)$ dominates. Here the nonequilibrium effects described by Eqs. (8) and (9) significantly increase the amplitudes of higher order harmonics as compared to the respective TDGL results.

Of particular interest is the dependence of the in-phase and out-of-phase parts of the amplitude of the main harmonic $j_m(t) = j_1 \sin\omega t + j_2 \cos\omega t$ on q_a, where j_2 determines the mean dissipative power $p = \omega q_a j_2/2$. Shown in Fig. 22 are steady-state oscillations of $j(t)$ at $\tau = 1$ and $\tau = 100$. At $q_a = 2^{-1/2}$ and $\tau = 100$, the current response is nearly in-phase with $q(t)$ but at $\tau = 1$ the current has dips when $q(t)$ is maximum. The latter comes from pair-breaking effects which mostly reduce the superfluid density and the supercurrent when $q(t)$ reaches maximum. This effect becomes more
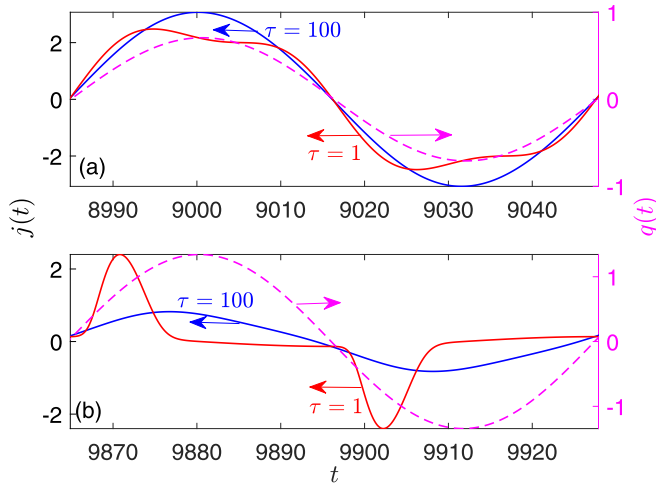
FIG. 22. Nonlinear current response $j(t)$ calculated at $q_a = 0.5\sqrt{2}$ and $q_a = 0.95\sqrt{2}$ for two values of $\tau = 1$ and $\tau = 100$ at $T = 0.9T_c$. At $\tau = 100$ the current is nearly in-phase with $q(t)$ at all q_a's. At $\tau = 1$ the current response at large q_a becomes almost evenly divided into the in-phase and out-of-phase parts.

pronounced for a larger amplitude $q_a = 0.95\sqrt{2}$ represented in Fig. 22(b). In this case $\psi(t)$ is much reduced during a considerable part of the AC period so $j_1 \ll j_2$ and the current response becomes nearly ohmic.

The dependencies of the in-phase $j_1(q_a)$ and out-of-phase $j_2(q_a)$ amplitudes of the current main harmonic on q_a are shown in Fig. 23 at $\tau = 1$ and $\tau = 100$. At $\tau = 100$ the response current is mostly in-phase with $q(t)$ up to the critical $q_a \approx \sqrt{2}$, while at $\tau = 1$, the out-of-phase part of $j_m(t)$ is essential and significantly increases with q_a and the supercurrent decreases.

B. Fixed $j(t)$

To calculate the Fourier harmonics of the dimensionless electric field $\varepsilon(t) = E(t)/E_0 = \partial q/\partial t$ with $E_0 = (2e\xi\tau_{GL})^{-1}$, we solved Eqs. (8)–(10) for $\psi(t)$ and $q(t)$ at a fixed AC current $j = j_a \sin \omega t$. Shown in Fig. 24 are the Fourier spectra $\varepsilon(\omega)$ at
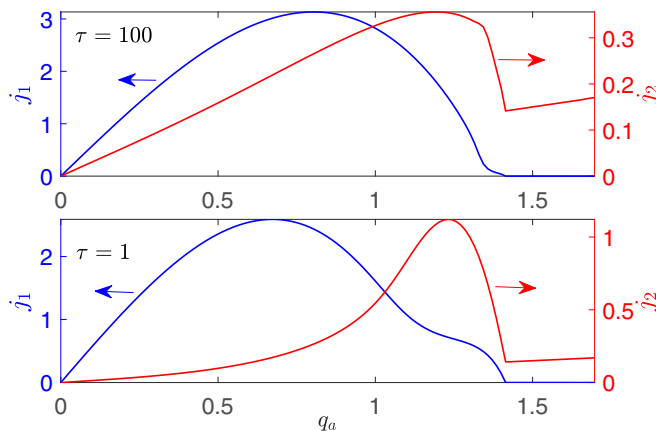

FIG. 23. The amplitudes $j_1(q_a)$ and $j_2(q_a)$ of the main current harmonic as functions of q_a calculated from Eqs. (8)–(10) at $T = 0.9T_c$ with $q(t) = q_a \sin \omega t$ at $\omega = 0.1$, $\tau = 1$, and $\tau = 100$.
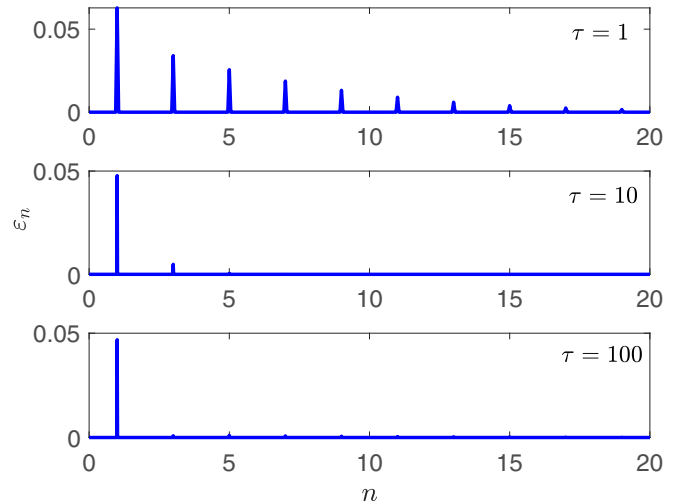

FIG. 24. Fourier spectra of the electric field $\varepsilon_n = \sqrt{\varepsilon_{1n}^2 + \varepsilon_{2n}^2}$ in response to the AC current $j = j_a \sin \omega t$ calculated from Eqs. (8)–(10) at $T = 0.9T_c$, $j_a = 0.77\sqrt{2}j_c$, $\omega = 0.1$, and different τ. The peaks in ε_n occur at the odd multiples of ω.

$j_a = 0.77\sqrt{2}j_c$, $\omega = 0.1$, and different τ. Like in the case of a fixed $q(t)$, the Fourier spectra of the electric field contain equidistant peaks at $\omega_n = n\omega$ with $n = 1, 3, 5, \ldots$, the amplitudes of higher order harmonics decreasing as τ increases.

Figure 25 shows the in-phase and out-of-phase amplitudes ε_1 and ε_2 of the main harmonic $\varepsilon_m(t) = \varepsilon_1 \sin \omega t + \varepsilon_2 \cos \omega t$ as functions of j_a at $\omega = 0.1$ and two values of $\tau = 1$ and $\tau = 100$. Here $\varepsilon_2(j_a)$ describing the superfluid response dominates at all j_a and is nearly linear in j_a, indicating that the dynamic differential resistivity $\rho_2 = \partial \varepsilon_2/\partial j_a$ is weakly dependent on j_a except for a sharp increase in a narrow region at $j_a \to j_d$ for both $\tau = 1$ and $\tau = 100$. By contrast, $\varepsilon_1(j_a)$ is linear in j_a at $j_a \lesssim j_d/2$ but then increases sharply as j_a approaches j_d. The differential resistivities $\rho_1(j_a) = \partial \varepsilon_1/\partial j_a$ and $\rho_2(j_a) = $
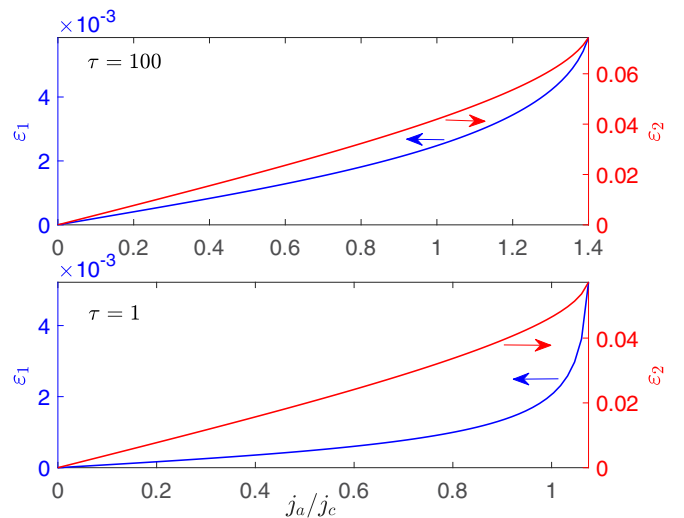

FIG. 25. The amplitudes $\varepsilon_1(j_a)$ and $\varepsilon_2(j_a)$ of the main electric field harmonic as functions of j_a calculated from Eqs. (8)–(10) at $T = 0.9T_c$ with $j(t) = j_a \sin \omega t$, $\omega = 0.1$, and $\tau = 1$ and $\tau = 100$.

FIG. 26. Differential resistivities ρ_1 and ρ_2 as functions of j_a calculated from Eqs. (8)–(10) at $T = 0.9T_c$ with $j(t) = j_a \sin \omega t$ at $\omega = 0.1$, $\tau = 1$, and $\tau = 100$.

FIG. 27. AC power $p = \varepsilon_1 j_a/2$ as functions of j_a calculated from Eqs. (8)–(10) at $T = 0.9T_c$ with $j(t) = j_a \sin \omega t$ at $\omega = 0.1$ for $\tau = 1$ and $\tau = 100$.
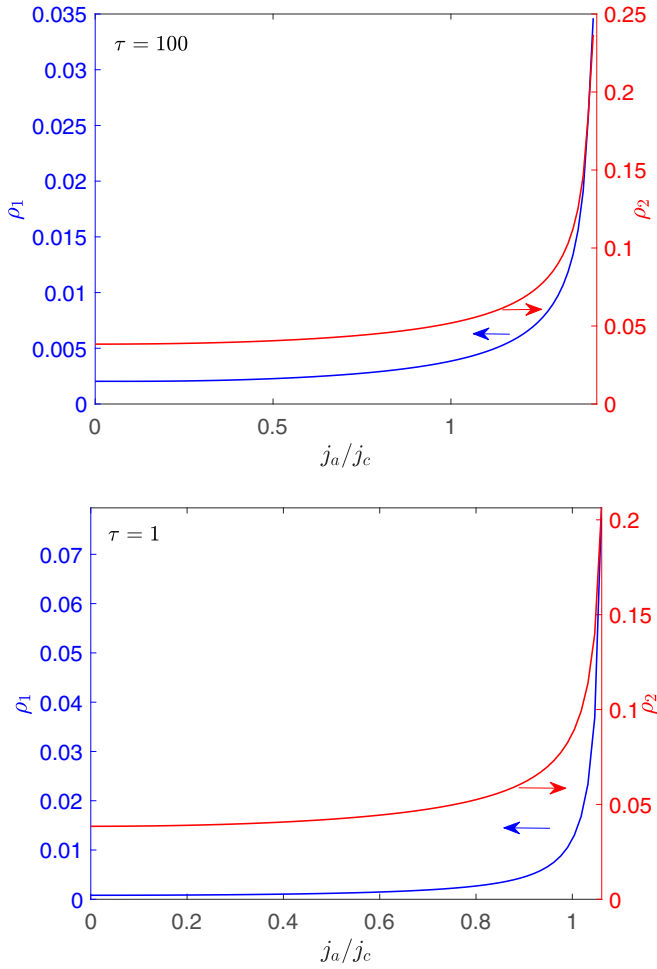
$\partial \varepsilon_2 / \partial j_a$ as well as the resulting dissipated power $p = P/P_0 = \varepsilon_1 j_a/2$ as functions of j_a where $P_0 = E_0 J_0$ are shown in Figs. 26 and 27, respectively. At $J > J_d$ the supercurrent density vanishes jumpwise, resulting in the ohmic response $J = \sigma_0 E$ in the normal state. Notice that both ρ_1 and ρ_2 turned out to be much smaller than the normal state resistivity $\rho_0 = 1/\sigma_0$ in the whole region of $0 < J_a < J_d$.

V. DISCUSSION

In this work we address the breakdown of superconductivity by strong rf currents at $\hbar\Omega \ll \Delta_0 \ll k_B T_c$. Here deviation of the quasiparticle distribution function $f(E, t)$ from equilibrium is controlled by the amplitude of rf current and the inelastic electron-phonon scattering time τ_E which can be much larger than τ_{GL} and the rf period $\Omega\tau_E \gg 1$. Because Eqs. (8)–(10) are applicable at $\hbar\Omega \ll k_B T_c$ [24–26], they do not describe a microwave stimulation of superconductivity which occurs at $\hbar\Omega \gtrsim k_B T$ [27]. Yet the kinetic equations (8)–(10) in which $\partial f/\partial E$ is replaced with its equilibrium value $\partial f_0/\partial E$ for a weak rf field [25,26] can have spurious solutions corresponding to stimulated superconductivity. We
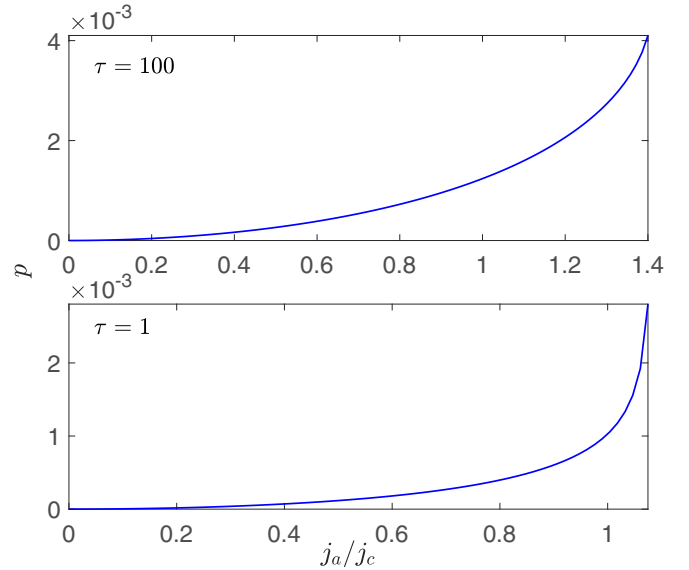
did observe these solutions of the linearized equations (8)–(10) but only at large rf amplitudes producing unphysical $\delta f(E, t) > 1$. The results presented above are obtained using the Larkin-Ovchinnikov form of Eqs. (8)–(10) which include the exact $\partial f/\partial E$ [24]. In this case the nonequilibrium correction $\delta f(E, t)$ was always smaller than 1 and no stimulated superconductivity was observed.

The temperature and frequency dependencies of Q_d and J_d calculated from either the TDGL equations or Eqs. (8)–(10) turned out to be similar. Namely, both Q_d and J_d tend to their respective static GL values at $\Omega\tau_E \ll 1$ and gradually increase with frequency, approaching the universal values $Q_d \to \sqrt{2}Q_c$ and $J_d \to \sqrt{2}J_c$ at $\max(\tau_{GL}, \tau_E)\Omega \gg 1$. The physics of this effect is rather transparent: at $\Omega\tau_E \gg 1$, the pair potential $\psi(t) = \langle\psi\rangle + \delta\psi(t)$ undergoes small-amplitude rapid oscillations of $\delta\psi(t)$ around a mean value $\langle\psi\rangle$ which is determined by quasistatic equations with the time-averaged $\langle Q^2\rangle = Q_a^2/2$. Thus, the solutions for the mean order parameter $\langle\psi\rangle$ disappear above the same pair-breaking critical value of $\langle Q^2\rangle$ as for a DC current. This result can also be used to evaluate the dynamic superheating field H_d at which the Meissner state in a large-κ superconductor becomes absolutely unstable:

$$H_d(T) \to H_s(T), \quad \Omega\tau_E(T) \ll 1, \tag{17}$$

$$H_d(T) \to \sqrt{2}H_s(T), \quad \Omega\tau_E(T) \gg 1, \tag{18}$$

$$H_s(T) = \left(\frac{\sqrt{5}}{3} + \frac{0.545}{\kappa}\right)H_c, \quad \kappa \gg 1, \tag{19}$$

where $H_s(T)$ is the DC superheating field at $T \approx T_c$ [65]. At $\kappa \gg 1$ the screening current density varies slowly over ξ, so $Q(x, t)$ and $\Delta(x, t)$ are nearly independent of the coordinate x perpendicular to the surface.

The relation between the dynamic superheating field $H_d(T)$ and the DC superheating field $H_s(T)$ at low temperatures $T \ll T_c$ and frequencies $\hbar\Omega \ll k_B T_c$ has not yet been calculated from a microscopic theory. Yet based on the known dependence of the quasiparticle gap ϵ_g on the mean free path at $H = H_s$ [16], we can make qualitative conclusions [66] regarding the essential effect of impurities on $H_d(T)$ at $T \ll T_c$. In the dirty limit $l \ll \xi_0$ at $T \ll T_c$, the quasiparticle gap $\epsilon_g(H)$ diminishes as the field increases but remains finite all the way to H_s at which $\epsilon_g(H_s) \approx 0.38\Delta_0$ [16], where $H_s = 0.84 H_c$ [14]. In this case the density of thermally activated quasiparticles remains exponentially small $n_{qp}(T) \lesssim n_0(\Delta_0/k_B T)^{1/2} \exp(-\epsilon_g/k_B T)$ in the entire field range of stability of the Meissner state, $0 < H < H_s$. A low frequency field $\hbar\Omega \ll \Delta_0$ can produce nonequilibrium quasiparticles which can affect dissipative kinetic coefficients and the surface resistance [66], but the effect of an exponentially small density of quasiparticles at $T \ll T_c$ on the dynamics of the superconducting condensate would be negligible, unlike the case of $T \approx T_c$ considered in this work. As a result, the condensate at $T \ll T_c$ reacts nearly instantaneously to the rf field with $\Omega \ll \Delta_0/\hbar$, despite slow kinetics of sparse quasiparticles, so the superconductivity would be destroyed under the same pair-breaking condition as in the absence of quasiparticles. Thus, the dynamic superheating field H_d of a dirty superconductor at $\hbar\Omega \ll \Delta_0$ and $T \ll T_c$ may be close to the static superheating field $H_s \approx 0.84 H_c$ even if $\Omega\tau_E \gg 1$.

For cleaner materials, the quasiparticle gap $\epsilon_g(H)$ vanishes before the DC depairing limit $H = H_s$ or $J = J_c$ is reached if $l \gtrsim 8.7\xi_0$ [16]. In this case the density of quasiparticles at $H = H_s$ is no longer negligible so their slow kinetics at $T \ll T_c$ may increase H_d relative to H_s even at $\hbar\Omega \ll \Delta_0$. A similar situation can also occur in superconductors with a nanostructured surface [62] or inhomogeneous density of impurities [67], where the quasiparticle gap at the surface can be reduced by both the current pair breaking and the proximity effect. Complex effects of impurities on the electron-phonon and electron-electron energy relaxation have been a subject of many experimental investigations in recent years [68–71].

Our calculations of a nonlinear electromagnetic response of a nonequilibrium superconducting state show that the amplitudes of higher order harmonics diminish as the quasiparticle energy relaxation time τ_E increases. Typically τ_E near T_c is about 2 orders of magnitude higher than τ_{GL}, except a narrow region of T very close to T_c. Given that strong disorder can significantly reduce τ_E [68–71], one could expect that generation of higher order harmonics and intermodulation effects would be more pronounced in dirty superconductors. The moderate dependence of the dynamic differential resistivity $\rho_2(j_a)$ which defines a nonequilibrium kinetic inductance on j_a shown in Fig. 26 is qualitatively similar to that of $\mathcal{L}_k(j_a)$ under the condition of the DC nonlinear Meissner effect [40,41,43,45]. At the same time, the dissipative differential resistivity $\rho_1(j_a)$ shown in Fig. 26 has a more pronounced dependence on j_a than $\rho_2(j_a)$. Both $\rho_1(j_a)$ and $\rho_2(j_a)$ have strong peaks as j_a approaches the dynamic depairing current density but remain much smaller than the normal state resistivity at low frequencies $\hbar\Omega \ll \Delta$. The nonlinearity of $\varepsilon(j_a)$ in a nonequilibrium state manifests itself in a strong dependence

of the rf dissipated power on the current amplitude, as shown in Fig. 27.

APPENDIX A: NONEQUILIBRIUM EQUATIONS

The equations obtained in Refs. [23–26] for a nonequilibrium dirty s-wave superconductor at $T \approx T_c$ and $\Omega \ll \Delta_0$ include the quasistationary Usadel equation:

$$\frac{D}{2}[\alpha(\nabla - 2ie\mathbf{A})^2\beta - \beta\nabla^2\alpha] = \left(\frac{1}{2\tau_E} - iE\right)\beta - \Psi\alpha, \quad \text{(A1)}$$

where the normal and anomalous retarded Green's functions $\alpha(E) = N_1(E) + iR_1(E)$ and $\beta(E) = N_2 + iR_2(E)$ satisfy $\alpha^2 + \beta^2 = 1$. Equation (A1) is supplemented by the kinetic equations for the odd $f(E)$ and even $f_1(E)$ distribution functions of quasiparticles:

$$D\nabla \cdot \left[(N_1^2 - R_2^2)\nabla\delta f\right] + 2DN_2 R_2 \mathbf{Q} \cdot \left(\nabla f_1 - e\frac{\partial f}{\partial E}\frac{\partial \mathbf{A}}{\partial t}\right)$$
$$-N_1\left(\frac{\partial}{\partial t} + \frac{1}{\tau_E}\right)\delta f = R_2\frac{\partial f}{\partial E}\frac{\partial|\Psi|}{\partial t}, \quad \text{(A2)}$$

$$D\nabla \cdot \left[(N_1^2 + N_2^2)\left(\nabla f_1 - e\frac{\partial f}{\partial E}\frac{\partial \mathbf{A}}{\partial t}\right)\right]$$
$$+ 2DN_2 R_2 \mathbf{Q} \cdot \nabla\delta f - N_1\left(\frac{\partial}{\partial t} + \frac{1}{\tau_E}\right)\left(f_1 + e\varphi\frac{\partial f}{\partial E}\right)$$
$$-N_2|\Psi|\left(2f_1 + \frac{\partial f}{\partial E}\frac{\partial\theta}{\partial t}\right) = 0, \quad \text{(A3)}$$

where $f = f_0 + \delta f$ and $f_0 = \tanh(E/2T)$.

The equations for $\Psi(\mathbf{r}, t) = \Delta\exp(-i\theta)$ and $\mathbf{J}(\mathbf{r}, t)$ are expressed in terms of $N_{1,2}$, $R_{1,2}$, δf and f_1 as follows [25,26]:

$$\left[\frac{\pi}{8T_c\epsilon}\frac{\partial}{\partial t} - \frac{1}{\Delta\epsilon}\int_0^\infty dE(R_2\delta f + iN_2 f_1)\right]\Psi$$
$$= \xi^2(\nabla - 2ie\mathbf{A})^2\Psi + \left(1 - \frac{\Delta^2}{\Delta_0^2}\right)\Psi, \quad \text{(A4)}$$

$$\mathbf{J} = \frac{\pi\sigma_0}{4eT_c}\Delta^2\mathbf{Q} + \frac{\sigma_0}{e}\int_0^\infty dE\left[(N_1^2 + N_2^2)\left(\nabla f_1 - e\frac{\partial f}{\partial E}\frac{\partial\mathbf{A}}{\partial t}\right)\right.$$
$$\left. + 2N_2 R_2 \mathbf{Q}\delta f\right]. \quad \text{(A5)}$$

If $\delta f(E, r, t)$ and $\Psi(r, t)$ vary slowly over τ_E, ξ, and $L_E = (D\tau_E)^{1/2}$, the derivatives in Eqs. (A2) and (A3) can be neglected. In this local equilibrium approximation Eqs. (A1)–(A5) reduce to Eqs. (3) and (4) [25,26].

If the spatial derivatives in Eqs. (A1)–(A5) are negligible we readily obtain $f_1 = -e\varphi\partial f/\partial E$ and $\Phi = -2e\varphi + \partial\theta/\partial t = 0$ from Eq. (A3), giving $\nabla f_1 - e(\partial f/\partial E)(\partial\mathbf{A}/\partial t) = 1/2(\partial f/\partial E)(\partial\mathbf{Q}/\partial t)$. In turn, Eq. (A1) reduces to the quartic

equation:

$$\alpha^4 - \mathcal{R}\alpha^3 + \mathcal{S}\alpha^2 + \mathcal{R}\alpha - \frac{\mathcal{R}^2}{4} = 0,$$

$$\mathcal{R} = \frac{2(u/\epsilon)^{1/2}(iE - 1/2\tau)}{q^2},$$

$$\mathcal{S} = \frac{\mathcal{R}^2}{4}\left[\frac{\psi^2}{(iE - 1/2\tau)^2} + 1\right] - 1. \qquad (A6)$$

The relevant solution of Eq. (A6) is given by

$$\alpha(E) = \frac{\mathcal{R}}{4} + \mathcal{E} + \frac{1}{2}\sqrt{-4\mathcal{E}^2 - 2\mathcal{A} - \frac{\mathcal{B}}{\mathcal{E}}}, \qquad (A7)$$

where

$$\mathcal{A} = \mathcal{S} - \frac{3\mathcal{R}^2}{8}, \quad \mathcal{B} = 8\mathcal{R} + 4\mathcal{R}\mathcal{S} - \frac{\mathcal{R}^3}{8},$$

$$\mathcal{C} = 2\mathcal{S}^3 + 27\mathcal{R}^2\mathcal{S} + 27\mathcal{R}^2 - \frac{27\mathcal{R}^4}{4},$$

$$\mathcal{D} = \left[\frac{1}{2}(\mathcal{C} + \sqrt{\mathcal{C}^2 - 4\mathcal{S}^6})\right]^{1/3},$$

$$\mathcal{E} = \frac{1}{2}\sqrt{-\frac{2\mathcal{A}}{3} + \frac{1}{3}\left(\mathcal{D} + \frac{\mathcal{S}^2}{\mathcal{D}}\right)}.$$

APPENDIX B: HIGH-FREQUENCY LIMIT, $\omega\tau \gg 1$

At high frequencies $\psi(t) = \psi + \delta\psi(t)$ has a small-amplitude oscillating component $\delta\psi(t) \ll \psi$ around a mean value ψ so that $\langle\delta\psi\rangle = 0$, where $\langle\cdots\rangle$ denotes time averaging. In this case Eqs. (6) and (7) can be solved by the standard methods which have been developed for dynamic equations with rapidly oscillating parameters [72,73].

1. Fixed $Q(t)$

For a fixed $q(t) = q_a\sin\omega t$ we expand Eq. (6) up to quadratic terms in $\delta\psi$ and average over the rf period:

$$r\dot{\psi} = (1 - \langle q^2\rangle)\psi - \psi^3 + \langle h\delta\psi\rangle - 3\langle\delta\psi^2\rangle\psi, \qquad (B1)$$

$$h(t) = \langle q^2\rangle - q^2(t) = \frac{q_a^2}{2}\cos 2\omega t, \qquad (B2)$$

where $r = (1 + 4\tau^2\psi^2)^{1/2}$, $\langle q^2\rangle = q_a^2/2$, and $\langle\delta\dot\psi\delta\psi\rangle = 0$.

The dynamic equation for $\delta\psi(t)$ is obtained by expanding Eq. (6) up to linear terms in $\delta\psi$:

$$r\psi\dot{\delta\psi} - g\delta\psi = h(t)\psi, \quad g = 1 - q_a^2/2 - 3\psi^2. \qquad (B3)$$

The solution of Eq. (B3) is then

$$\delta\psi(t) = A\cos 2\omega t + B\sin 2\omega t, \qquad (B4)$$

$$A = -\frac{q_a^2 g\psi}{2(4\omega^2 r^2 + g^2)}, \quad B = \frac{q_a^2\omega r\psi}{4\omega^2 r^2 + g^2}. \qquad (B5)$$

From Eqs. (B1) and (B4) we obtain the following self-consistency equation for $\psi(t)$:

$$r\dot{\psi} = \left(1 - \frac{q_a^2}{2}\right)\psi - \psi^3 + \frac{q_a^2 A}{4} - \frac{3}{2}\psi(A^2 + B^2). \qquad (B6)$$

At $4\omega^2 r^2 \gg g^2$, Eqs. (B5) and (B6) reduce to

$$r\dot{\psi} = \left(1 - \frac{q_a^2}{2}\right)\left(1 - \frac{q_a^4}{32\omega^2 r^2}\right)\psi - \psi^3. \qquad (B7)$$

Hence, the mean steady-state ψ is given by

$$\psi = \left(1 - \frac{q_a^2}{2}\right)^{1/2}\left(1 - \frac{q_a^4}{64\omega^2 r^2}\right). \qquad (B8)$$

This state is stable with respect to small perturbations of $\psi(t)$ if $q_a < q_d = \sqrt{2}$.

2. Fixed $J(t)$

For a fixed $j(t) = j_a\sin\omega t$, we linearize Eq. (7) with respect to an oscillating correction $\delta\psi(t) \ll 1$:

$$j_a\sin\omega t = qu\psi^2 + 2u\psi q\delta\psi + \dot{q}. \qquad (B9)$$

Setting here $q(t) = q_1\sin\omega t + q_2\cos\omega t$ and $\delta\psi = A\cos 2\omega t + B\sin 2\omega t$, we obtain $\langle q\delta\psi\rangle = 0$, and $q(t) = -(j_a/u\psi^2)\sin\omega t$ in leading order in $\omega/u \ll 1$ and $(\omega r)^{-2} \ll 1$. Substituting this $q(t)$ into Eq. (6) and averaging gives the equation for the mean $\psi(t)$:

$$(1 + 4\tau^2\psi^2)^{1/2}\dot{\psi} = \left(1 - \frac{j_a^2}{2u^2\psi^4}\right)\psi - \psi^3. \qquad (B10)$$

The right-hand side of Eq. (B10) has the GL form for a fixed current except that the time averaging of $\langle q^2(t)\rangle = j_a^2/2u^2\psi^4$ reduces the current pair-breaking term in half as compared to the DC current. As a result,

$$j_a^2 = 2u^2\psi^4(1 - \psi^2). \qquad (B11)$$

Stability of the above steady state with respect to slow perturbations $\psi_1(t)$ can be addressed by setting $\psi(t) = \psi + \psi_1(t)$ and linearizing Eq. (B10) with respect to ψ_1:

$$r\dot{\psi}_1 = \left[1 + \frac{3j_a^2}{2u^2\psi^4} - 3\psi^2\right]\psi_1. \qquad (B12)$$

Hence, $\psi_1 \propto \exp(\gamma t)$, where the decrement γ is given by

$$\gamma = \frac{2}{r}(2 - 3\psi^2). \qquad (B13)$$

Here j_a^2 in Eq. (B12) was expressed in terms of ψ^2 using Eq. (B11). This state becomes unstable ($\gamma > 0$) at $j_d = \sqrt{2}j_c$ for which $j_a(\psi)$ reaches maximum at $\psi^2 = 2/3$.

[1] M. Tinkham, *Introduction to Superconductivity*, 2nd ed. (McGraw-Hill, New York, 1995).

[2] V. L. Ginzburg, Dokl. Akad. Nauk SSSR **118**, 464 (1958) [Sov. Phys.-Doklady **3**, 102 (1958)].

[3] R. H. Parmenter, RCA Rev. **26**, 23 (1962).

[4] J. Bardeen, Rev. Mod. Phys. **34**, 667 (1962).

[5] K. Maki, Prog. Theor. Phys. **29**, 333 (1963).

[6] K. Maki, Gapless superconductivity, in *Superconductivity*, edited by R. D. Parks (Marcel Dekker, New York, 1969).

[7] M. Yu. Kupriyanov and V. F. Lukichev, Fiz. Nizk. Temp. **6**, 445 (1980) [Sov. J. Low Temp. Phys. **6**, 210 (1980)].

[8] E. J. Nicol and J. P. Carbotte, Phys. Rev. B **43**, 10210 (1991).

[9] M. N. Kunchur, D. K. Christen, C. E. Klabunde, and J. M. Phillips, Phys. Rev. Lett. **72**, 752 (1994).

[10] N. M. Kunchur, J. Phys. Condens. Matter **16**, R1183 (2004).

[11] V. Rouco, C. Navau, N. Del-Valle, D. Massarotti, G. P. Papari, D. Stornaiuolo, X. Obradors, T. Puig, F. Tafuri, A. Sanchez, and A. Palau, Nano Lett. **19**, 4174 (2019).

[12] J. Matricon and D. Saint-James, Phys. Lett. A **24**, 241 (1967).

[13] S. J. Chapman, SIAM J. Appl. Math. **55**, 1233 (1995).

[14] V. P. Galaiko, Zh. Eksp Teor. Fiz. **50**, 717 (1966) [Sov. Phys. JETP **23**, 475 (1966)].

[15] G. Catelani and J. P. Sethna, Phys. Rev. B **78**, 224509 (2008).

[16] F. P.-J. Lin and A. Gurevich, Phys. Rev. B **85**, 054513 (2012).

[17] W. Belzig, C. Bruder, and G. Schön, Phys. Rev. B **53**, 5727 (1996).

[18] A. L. Fauchere and G. Blatter, Phys. Rev. B **56**, 14102 (1997).

[19] W. Belzig, C. Bruder, and A. L. Fauchere, Phys. Rev. B **58**, 14531 (1998).

[20] A. V. Galaktionov and A. D. Zaikin, Phys. Rev. B **67**, 184518 (2003).

[21] N. B. Kopnin, *Theory of Nonequilibrium Superconductivity* (Oxford University Press, Oxford, England, 2001).

[22] S. B. Kaplan, C. C. Chi, D. N. Langenberg, J. J. Chang, S. Jafarey, and D. J. Scalapino, Phys. Rev. B **14**, 4854 (1976).

[23] A. Schmid and G. Schön, J. Low Temp. Phys. **20**, 207 (1975).

[24] A. I. Larkin and Yu. N. Ovchinnikov, Zh. Eksp. Teor. Fiz. **73**, 299 (1977) [Sov. Phys. JETP **46**, 1 (1977)].

[25] L. Kramer and R. J. Watts-Tobin, Phys. Rev. Lett. **40**, 1041 (1978).

[26] R. J. Watts-Tobin, Y. Krähenbühl, and L. Kramer, J. Low Temp. Phys. **42**, 459 (1981).

[27] G. M. Eliashberg and B. I. Ivlev, *Nonequilibrium Superconductivity*, edited by D. N. Langenberg and A. I. Larkin (Elsevier, Amsterdam, 1986), p. 211.

[28] P. Fulde, Phys. Rev. **137**, A783 (1965).

[29] A. Anthore, H. Pothier, and D. Esteve, Phys. Rev. Lett. **90**, 127001 (2003).

[30] P. K. Day, H. G. Leduc, B. A. Mazin, A. Vayonakis, and J. Zmuidzinas, Nature (London) **425**, 817 (2003).

[31] J. Zmuidzinas, Rev. Condens. Matter Phys. **3**, 169 (2012).

[32] H. Padamsee, J. Knobloch, and T. Hays, *RF Superconductivity for Accelerators* (John Wiley, New York, 1998).

[33] A. Gurevich, Supercond. Sci. Technol. **30**, 034004 (2017).

[34] T. Yogi, G. J. Dick, and J. E. Mercereau, Phys. Rev. Lett. **39**, 826 (1977).

[35] S. Posen, N. Valles, and M. Liepe, Phys. Rev. Lett. **115**, 047001 (2015).

[36] W. J. Skocpol, M. R. Beasley, and M. Tinkham, J. Low Temp. Phys. **16**, 145 (1974).

[37] B. I. Ivlev and N. B. Kopnin, Adv. Phys. **33**, 47 (1984).

[38] R. Tidecks, *Current-Induced Nonequilibrium Phenomena in Quasi-One-Dimensional Superconductors* (Springer, Berlin, 2006), Vol. 121.

[39] D. Y. Vodolazov and F. M. Peeters, Phys. Rev. B **81**, 184521 (2010).

[40] S. K. Yip and J. A. Sauls, Phys. Rev. Lett. **69**, 2264 (1992); D. Xu, S. K. Yip, and J. A. Sauls, Phys. Rev. B **51**, 16233 (1995).

[41] T. Dahm and D. J. Scalapino, J. Appl. Phys. **81**, 2002 (1997); Phys. Rev. B **60**, 13125 (1999).

[42] W. Hu, A. S. Thanawalla, B. J. Feenstra, F. C. Wellstood, and S. M. Anlage, Appl. Phys. Lett. **75**, 2824 (1999).

[43] M. R. Li, P. J. Hirschfeld, and P. Wölfle, Phys. Rev. Lett. **81**, 5640 (1998); Phys. Rev. B **61**, 648 (2000).

[44] D. E. Oates, J. Supercond. Novel Magn. **20**, 3 (2007).

[45] N. Groll, A. Gurevich, and I. Chiorescu, Phys. Rev. B **81**, 020504(R) (2010).

[46] R. Meservey and P. M. Tedrow, J. Appl. Phys. **40**, 2028 (1969).

[47] J. R. Clem and E. H. Brandt, Phys. Rev. B **72**, 174511 (2005).

[48] G. Via, C. Navau, and A. Sanchez, J. Appl. Phys. **113**, 093905 (2013).

[49] A. J. Annunziata, D. F. Santavicca, L. Frunzio, G. Catelani, M. J. Rooks, A. Frydman, and D. E. Prober, Nanotechnology **21**, 445202 (2010).

[50] K. Enpuku, H. Moritaka, H. Inokuchi, T. Kisu, and M. Takeo, Jpn. J. Appl. Phys. **34**, L675 (1995).

[51] D. E. McCumber and B. I. Halperin, Phys. Rev. B **1**, 1054 (1970).

[52] K. Yu. Arutyunov, D. S. Golubev, and A. D. Zaikin, Phys. Rep. **464**, 1 (2008).

[53] J. E. Mooij and Yu. V. Nazarov, Nat. Phys. **2**, 169 (2006).

[54] M. Sahu, M-H. Bae, A. Rogachev, D. Pekker, T-C. Wei, N. Shah, P. M. Goldbart, and A. Bezryadin, Nat. Phys. **5**, 503 (2009).

[55] R. Rangel and L. Kramer, J. Low Temp. Phys. **74**, 163 (1989).

[56] D. Y. Vodolazov, A. Elmuradov, and F. M. Peeters, Phys. Rev. B **72**, 134509 (2005).

[57] L. Kramer and R. Rangel, J. Low Temp. Phys. **57**, 391 (1984).

[58] N. W. Ashkroft and N. D. Mermin, *Solid State Physics* (Holt, Rinehart and Winston, Philadelphia, 1976).

[59] J. P. Carbotte, Rev. Mod. Phys. **62**, 1027 (1990).

[60] R. C. Dynes, V. Narayanamurti, and J. P. Garno, Phys. Rev. Lett. **39**, 229 (1977).

[61] J. Zasadzinski, Tunneling spectroscopy of conventional and unconventional superconductors. in *The Physics of Superconductors*, edited by K. H. Bennemann and J. B. Ketterson (Springer, New York, 2003), Chap. 15, p. 591.

[62] T. Kubo and A. Gurevich, Phys. Rev. B **100**, 064522 (2019).

[63] W. E. Schiesser, *The Numerical Method of Lines: Integration of Partial Differential Equations* (Academic, San Diego, 1991).

[64] L. F. Shampine and M. K. Gordon, *Computer Solution of Ordinary Differential Equations: The Initial Value Problem* (W. H. Freeman, San Francisco, 1975).

[65] M. K. Transtrum, G. Catelani, and J. P. Sethna, Phys. Rev. B **83**, 094505 (2011).

[66] A. Gurevich, Phys. Rev. Lett. **113**, 087001 (2014).

[67] V. Ngampruetikorn and J. A. Sauls, Phys. Rev. Res. **1**, 012015(R) (2019).

[68] A. Leo, G. Grimaldi, R. Citro, A. Nigro, S. Pace, and R. P. Huebener, Phys. Rev. B **84**, 014536 (2011).

[69] M. V. Sidorova, A. G. Kozorezov, A. V. Semenov, Yu. P. Korneeva, M. Yu. Mikhailov, A. Yu. Devizenko, A. A. Korneev, G. M. Chulkova, and G. N. Goltsman, Phys. Rev. B **97**, 184512 (2018).

[70] L. Zhang, L. You, X. Yang, J. Wu, C. Lv, Q. Guo, W. Zhang, H. Li, W. Peng, Z. Wang, and X. Xie, Sci. Rep. **8**, 1486 (2018).

[71] Yu. P. Korneeva, N. N. Manova, I. N. Florya, M. Yu. Mikhailov, O. V. Dobrovolskiy, A. A. Korneev, and D. Yu. Vodolazovs, Phys. Rev. Appl. **13**, 024011 (2020).

[72] L. D. Landau and E. M. Lifshitz, *Mechanics* (Elsevier, Boston, 1976).

[73] N. N. Bogoliubov and Y. A. Mitropolski, *Asymptotic Methods in the Theory of Nonlinear Oscillations* (Gordon and Breach, New York, 1961).